Molecular Mobility of Amorphous S-Flurbiprofen: A Dielectric Relaxation Spectroscopy Approach

ARTICLE *in* MOLECULAR PHARMACEUTICS · NOVEMBER 2013

Impact Factor: 4.38 · DOI: 10.1021/mp4002188 · Source: PubMed

5 AUTHORS, INCLUDING:

María Teresa Viciosa
Technical University of Lisbon
30 PUBLICATIONS **337** CITATIONS

SEE PROFILE

molecular pharmaceutics

Article

pubs.acs.org/molecularpharmaceutics

Molecular Mobility of Amorphous *S*-Flurbiprofen: A Dielectric Relaxation Spectroscopy Approach

A. C. Rodrigues,[†] M. T. Viciosa,[‡] F. Danède,[§] F. Affouard,[§] and N. T. Correia*[,†,§]

[†]REQUIMTE/CQFB, Departamento de Química, Faculdade de Ciências e Tecnologia, Universidade Nova de Lisboa, 2829-516 Caparica, Portugal

[‡]CQFM − Centro de Química-Física Molecular and IN − Institute of Nanoscience and Nanotechnology, Instituto Superior Técnico, Universidade de Lisboa, Avenida Rovisco Pais, 1049-001 Lisboa, Portugal

[§]Unité Matériaux et Transformation (UMET), UMR CNRS 8207, UFR de Physique, BAT P5, Université Lille 1, 59655 Villeneuve d'Ascq, France

ABSTRACT: Amorphous *S*-flurbiprofen was obtained by the melt quench/cooling method. Dielectric measurements performed in the isochronal mode, conventional and temperature modulated differential scanning calorimetry (TMDSC) studies showed a glass transition, recrystallization, and melting. The different parameters characterizing the complex molecular dynamics of amorphous *S*-flurbiprofen that can have influence on crystallization and stability were comprehensively characterized by dielectric relaxation spectroscopy experiments (isothermal mode) covering a wide temperature (183 to 408 K) and frequency range (10^{-1} to 10^{6} Hz): width of the α-relaxation (β_{KWW}), temperature dependence of α-relaxation times (τ_α), fragility index (m), relation of the α-relaxation with the β-secondary relaxation, and the breakdown of the Debye−Stokes−Einstein (DSE) relationship between the structural relaxation time and dc-conductivity (σ_{dc}) at deep undercooling close to T_g. The β-relaxation, observed in the glassy as well as in the supercooled state was identified as the genuine Johari−Goldstein process, attributed to localized motions and regarded as the precursor of the α-relaxation as suggested in the coupling model. A separation of about 6 decades between the α- and β-relaxation was observed at T_g; this decoupling decreased on increasing temperature, and both processes merged at $T_{\alpha\beta}$ = 295 K. The temperature dependence of the α-relaxation time, τ_α, was described by two Vogel−Fulcher−Tammann−Hesse equations, which intercept at a crossover temperature, T_B = 290 K, close to the splitting temperature between the α- and β-relaxation. From the low temperature VFTH equation, a T_g^{DRS} = 265.2 was estimated (at τ_α =100 s) in good agreement with the calorimetric value ($T_{g,onset,TMDSC}$ = 265.6 K), and a fragility or steepness index m = 113 was calculated allowing to classify *S*-flurbiprofen as a fragile glass former. The α-relaxation spectra were found to be characterized by a relatively large degree of nonexponentiality (β_{KWW} = 0.52). A breakdown of the DSE $\log_{10}\sigma_{dc} - \log_{10}\tau$ relation was observed revealing an enhancement of translational ionic motions in comparison with the orientational molecular motions as the glass transition temperature T_g is approached from above.

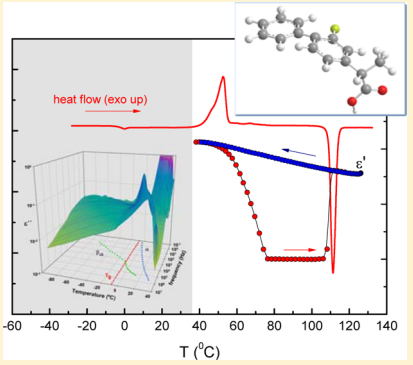

KEYWORDS: *dielectric relaxation spectroscopy, glass transition, fragility, Johari−Goldstein β-relaxation, flurbiprofen, ibuprofen, physical stability*

1. INTRODUCTION

Until now, many substances of pharmacy have been developed especially in the crystalline state for obvious reasons of stability. However, either by accident or design, they may also exist in a total or partially amorphous state. Because of its higher Gibbs free energy, the amorphous form of a drug often shows an improved solubility and accelerated dissolution and bioavailability promoting therapeutic activity when compared to its crystalline state.[1−6] Development of active substances in the amorphous form thus offers an interesting route and has motivated a strong interest in the past decade. However, these forms are inherently unstable physically, which is a significant concern from a pharmaceutical perspective. If the molecular motions causing this instability are not arrested over a time scale meaningful for pharmaceutical applications, important changes in some of the physicochemical properties[1,7,8] of the drug may occur. For example, significant molecular mobility can persist in the glass (below the glass transition temperature, T_g) promoting occurrence of crystallization from the amorphous solid.[9−13] In this context, the knowledge of the time scales and temperature dependencies of molecular motions is particularly important for a stable storage and the shelf life of amorphous pharmaceuticals.[14]

Broadband dielectric relaxation spectroscopy (DRS) is a powerful, noninvasive tool to assess in situ the dynamical behavior in the vitreous and the supercooled liquid state of glass formers.[15] Relevant information about the different

Received: April 13, 2013
Revised: October 2, 2013
Accepted: November 11, 2013
Published: November 11, 2013

molecular dynamics can be obtained through the study of dipolar reorientations covering a wide time scale (10^5 s to 10^{-12} s) and temperature range. In fact, the DRS technique enables the study of several processes, from slow hindered cooperative molecular motions to relatively fast reorientations of small molecules or side groups, as well as ionic and protonic conductivity. Dielectric spectroscopy is widely used in the study of complex systems in materials science and is attracting increasing attention as a powerful tool of characterization of pharmaceutical materials.[16,17] In particular, DRS has been recently used for characterizing the dynamics in viscous supercooled liquid and vitreous forms of active pharmaceutical ingredients like the well-known indomethacin,[18−20] acetaminophen,[21] aspirin,[22,23] fananserine,[24] nicotine,[25] ibuprofen,[23,26−29] celexocib,[13,30] and pharmaceutical molecular alloys based on nifedipine, aspirin, and acetaminophen,[31−35] among other pharmaceutical drugs.[36−41] It was found that the crystallization of the above-mentioned pharmaceutical drugs can be circumvented on cooling from the melt, and they present similar properties as conventional glass forming materials,[42−45] both in the supercooled liquid and glassy form. The same phenomenology thus applies to the dynamical behavior of systems of pharmaceutical interest. Some of the most relevant aspects characterizing the complex dynamics of glass formers obtained from DRS can play a significant influence on the crystallization processes and stability of pharmaceuticals: (i) the non-Arrhenius behavior of the α-relaxation time on approaching T_g from above, quantified by the fragility index; (ii) the nonexponential character described by the stretching parameter β_{KWW}; (iii) correlation between the α-relaxation and the Johari−Goldstein secondary relaxation that persists in the glassy state; and (iv) breakdown of the Debye−Stokes−Einstein relationship on approaching T_g. A brief description is given below.

(i) The temperature dependence of the relaxation time, $\tau_\alpha(T)$, for the structural relaxation, the so-called α-relaxation (dynamic glass transition), that is the dominant process in the supercooled state, usually shows deviation from the Arrhenius behavior being described by the empirical Vogel−Fulcher−Tammann−Hesse (VFTH) equation close to T_g:[46−48]

$$\tau(T) = \tau_\infty \exp\left(\frac{B}{T - T_0}\right) \tag{1}$$

where τ_∞, B, T_0 are empirical parameters characteristic of a material. τ_∞ is the limiting relaxation time at high temperature corresponding to a vibrational frequency ($\sim 10^{-11}$ to 10^{-14} s), and T_0 is the so-called Vogel temperature being found about 50 to 70 degrees below T_g. The glass transition temperature T_g is typically defined as the temperature at which $\tau_\alpha(T) \approx 100$ s and is usually close to the value determined by calorimetry. Equation 1 describes the extreme slowing down of molecular motions upon cooling the supercooled liquid, in such a way that τ_α increases more rapidly as the temperature decreases becoming formally infinity at a finite temperature $T = T_0$. Stated otherwise, T_0 is the temperature where mobility associated with the dynamic glass transition, often connected to instabilities, becomes zero.

The Vogel temperature can be taken for estimation of the Kauzmann temperature, T_K,[49] the hypothetical temperature at which the extrapolated entropy of the supercooled liquid would be equal to the entropy value of the crystal. Shamblin et al.[14] estimated the relaxation times in several real glasses (including indomethacin) as being on the order of 3−5 years at temperatures near T_K. Assuming that crystallization couples with the rate of molecular motions in glasses, the storage of amorphous materials at temperatures below T_0 (or T_K) expected ensuring their physical stability for several months or even years.[14] Nevertheless one must be careful when using T_0 as an indicator for a safe storage since it is implicit that besides the structural relaxation other molecular mobilities are also kinetically frozen below T_0, which is not always the case; evidence of crystallization (or at least nucleation) have been reported for some amorphous pharmaceuticals when stored at temperatures much below T_g.[12]

The degree of deviation from Arrhenius-type temperature dependence near T_g provides a useful classification of glass formers.[50−53] Materials are called fragile if their temperature dependence of τ_α markedly deviates from the Arrhenius behavior and strong if it is close to the latter. In other words, fragility indicates how strongly the relaxation time changes as T_g is approached from temperatures above the glass transition.

A quantitative measure of the fragility can be obtained from the fragility or steepness index m according the following equation:

$$m = \left.\frac{d \log_{10} \tau(T)}{d(T_g/T)}\right|_{T=T_g} \tag{2}$$

Fragility values typically range between $m = 16$ for strong systems and $m \approx 200$ (ref 52) for fragile systems where a marked deviation from an Arrhenius dependence occurs induced by high cooperativity molecular rearrangements.[54] Fragility is one central parameter describing glassy dynamics and reflecting the stability of a liquid structure to temperature changes in the supercooled state.[43] Fragility is also correlated with the nonexponentiality of the relaxation function of the α-relaxation[53] where the nonexponentiality can be associated to intermolecular cooperativity.

Knowledge of the fragility index is of interest for the pharmaceutical field concerning the stability of amorphous drugs.[55] From the point of view of structural stability against temperature fluctuations, strong glass formers are expected to be more physically stable than fragile; the properties of a more fragile material will change significantly with small variations of temperature during storage. If stabilization of an amorphous material by reduction of the temperature is concerned, fragility can be used to estimate the degree of undercooling necessary for the relaxation time to exceed the expected storage time.[55] In this situation, a more fragile glass former, exhibiting a stronger dependence on temperature, might be preferred.

(ii) In many supercooled liquids the α-relaxation function, $\phi(t)$ (in the time (t) domain), becomes increasingly nonexponential as T_g is approached from above being often described by the empirical Kohlrausch−Williams−Watts (KWW) stretched exponential expression:[56,57]

$$\phi(t) = \exp\left[-\left(\frac{t}{\tau_{KWW}}\right)^{\beta_{KWW}}\right] \tag{3}$$

where τ_{KWW} is a characteristic relaxation time and β_{KWW} ($0 < \beta_{KWW} \leq 1$) is the stretching parameter that quantifies the extent to which the relaxation process deviates from the exponential (Debye) decay. For the Debye-type relaxation $\beta_{KWW} = 1$, the spectrum has a single relaxation time, and the peak breath (in

dx.doi.org/10.1021/mp4002188 | Mol. Pharmaceutics 2014, 11, 112−130

the frequency domain) is 1.14 decades. A smaller β_{KWW} denotes a broader relaxation peak, i.e., a broader and asymmetric distribution of relaxation times. Böhmer et al.,[52] using data for many glass formers, proposed a broad correlation between the non-Arrhenius and the non-Debye behavior of the α-relaxation described by a linear relationship between the fragility index m and β_{KWW}:

$$m = 250(\pm 30) - 320\beta_{KWW} \quad (4)$$

Accordingly, fragile glass formers having high values of m should be characterized by a low value of β_{KWW} in the vicinity of T_g, i.e., a dielectric relaxation function with a high level of nonexponentiality; strong materials with lower m should have higher values of β_{KWW}.

Shamblin et al.[58] suggested that the distribution of molecular motions described by the β_{KWW} parameter can play a role in the physical or chemical stability of amorphous pharmaceutics. A narrower distribution of the α-relaxation times (higher β_{KWW} value) would be an indication of a smaller tendency of the amorphous drug to crystallization; a lower β_{KWW} value would indicate a greater propensity to crystal nucleation due to the faster, localized molecular motions.[45,59]

(iii) The presence of one or more secondary relaxations preceding in time the structural α-relaxation is another universal feature of supercooled liquids.[44,45] These processes are usually named as β, γ, etc., in order of decreasing relaxation time (increasing frequency or decreasing temperature). Contrary to the main relaxation associated with cooperative molecular motions, secondary relaxations are typical of faster, noncooperative, local mobility that can remain kinetically unfrozen at temperatures well below T_g. These are thermally activated processes; the relaxation times, $\tau_{\beta,\gamma,...}(T)$, follow Arrhenius-type temperature dependence below T_g. Among several molecular mechanisms that may be at the origin of secondary relaxations of different materials, the β-process that involves intermolecular degrees of freedom is of particular relevance to the glass transition phenomena. It is the so-called Johari–Goldstein (JG) β-relaxation[60] that in glass formers of small molecules corresponds to the rotation of the molecule as a whole,[61,62] and it is regarded as a precursor of the cooperative α-relaxation. According to the coupling model (CM),[61] the JG β-process relaxation time, τ_{JG}, is correlated with that of the α-process, τ_α, by

$$\tau_{JG}(T) \approx \tau_0(T) = t_c^{\,n}[\tau_\alpha(T)]^{1-n} \quad (5)$$

where τ_0 is the relaxation time of the primitive process postulated in the CM; the coupling parameter $n = 1 - \beta_{KWW}$, and τ_α is the relaxation time of the KWW function (τ_{KWW} in eq 3); t_c is a time characterizing the crossover from localized to cooperative fluctuations found to be close to 2×10^{-12} s for molecular glass-formers.[63] The JG β-relaxation has been found well resolved in dielectric spectra of several pharmaceutical glass formers, namely, aspirin,[22] ibuprofen,[27] fananserine,[24] celecoxib,[13] and telmisartan.[38]

Recent literature reviews focusing on the potential impacts of local molecular mobility originating from secondary relaxations on the physical and chemical stability of systems of pharmaceutical interest are given in ref 45 and references therein. It is recognized that the JG β-relaxation plays an important role in the stability of amorphous pharmaceuticals. In particular, in the glassy state at temperatures well below T_g, when cooperative motions (α-relaxation) are completely frozen, the JG β-relaxation may be responsible for the origin of nucleation and crystallization instabilities.

(iv) Another common feature of the dynamical behavior of glass forming systems is the breakdown of the well-known Stokes–Einstein (SE) and Debye–Stokes relationships when the temperature is decreased approaching T_g (often both are combined and referred to as Debye–Stokes–Einstein equation, DSE). A detailed description of this topic and theoretical explanations can be found in several review articles and recent books and references therein.[43,45,64−67] Briefly, these relationships apply to translational and rotational molecular transport, respectively. For low viscosity liquids, a simple proportionality is postulated between the translational (rotational) self-diffusion coefficient D_t (D_r) and the inverse of viscosity, η, i.e., $D_t \propto \eta^{-1}$ ($D_r \propto \eta^{-1}$). However, a decoupling of self-diffusion dynamics and viscosity has been observed in interacting systems at low temperatures near the glass transition. For example, in several deeply supercooled fragile liquids, the temperature dependence of D_t has been found to be significantly weaker than η^{-1}. The Stokes–Einstein equation breaks down, and a fractional SE relationship applies: $D_t \propto \eta^{-\xi}$ with $0 < \xi < 1$, which indicates that there is enhancement of translational diffusion in comparison with viscous flow. The change in the temperature dependence behavior of the translational diffusion and viscosity usually occurs close to the so-called dynamical crossover temperature $T_B \approx 1.2T_g$.

The self-diffusion coefficient D_t characterizes the transport phenomenon within a liquid, and it has been found that it is responsible for the mass transport for crystallization.[65,68] Below T_B the crystal growth kinetics are faster than predicted from viscosity data being controlled mainly by the translational diffusion, whereas above T_B viscosity or structural relaxation is the governing factor.[65] Moreover, it has been found that the decoupling between crystal growth kinetics and viscosity near T_g systematically depends on the fragility index m of the glass forming liquid: a greater decoupling, faster crystallization process, is observed for more fragile liquids.[68] For moderately or highly fragile organic liquids, the self-diffusion coefficient is thus a better predictor of crystal growth rates.[67] The coupling model[53,69] predicts that the decoupling between diffusion from viscosity is related to the coupling parameter $n = 1 - \beta_{KWW}$ (or anticorrelation with the Kohlrausch parameter β_{KWW}): the stronger the decoupling, the stronger the decoupling between crystal growth and viscosity near T_g. Thus, a larger coupling parameter (i.e., larger dispersion of the α-relaxation, smaller β_{KWW}) leads to faster crystallization rate at T_g. The coupling parameter correlates usually although not always with fragility (β_{KWW} anticorrelates with fragility, eq 4).

The decoupling of different dynamic variables is a general phenomenon not only restricted to translational and rotational diffusion or viscosity.[45] Dielectric spectroscopy provides simultaneous measurements of a rotational dynamic component (dielectric orientational relaxation; α-relaxation time τ_α) and a translational component (dc conductivity, σ_{dc}) in the presence of an electric field, over a broad dynamic range.[70,71] The dc conductivity is detected at lower frequencies (higher temperatures) than the α-relaxation, and it is originating from the translation of trace mobile ions and/or intrinsic proton diffusion along hydrogen bonds.[23,31,32]

When the two dynamics are coupled, a relationship exists between the temperature dependence of the dc conductivity and the α-relaxation time of the liquid:[66,70,71]

$$\sigma_{dc}(T) \propto 1/\tau_{\alpha}(T) \quad (6)$$

Accordingly, σ_{dc} varies linearly with $1/\tau_{\alpha}$, i.e., the product $\sigma_{dc}(T)\tau_{\alpha}(T)$ remains constant with changing temperature. This relationship was derived taking into account the Nernst−Einstein equation that relates σ_{dc} with the diffusion coefficient of ions, D_i ($\sigma_{dc} \propto D_i$) and the Stokes−Einstein and Debye−Stokes relationships; eq 6 is also commonly known as the Debye−Stokes−Einstein (DSE) relationship. Nevertheless, as observed for other dynamic properties, the breakdown of this relationship is often observed in glass-forming materials[66,70−73] as the temperature is lowered toward the glass transition temperature, and an empirical fractional DSE (FDSE) equation is needed to describe the experimental data:

$$\sigma_{dc}(T) \propto 1/\tau_{\alpha}(T)^{x} \quad (\text{or } \sigma_{dc}(T)\tau_{\alpha}(T)^{x} \cong \text{const}) \quad (7)$$

with the exponent $0 < x < 1$. This event is known as decoupling of ionic diffusion from dielectric relaxation. In a recent study of several polymers,[74] it was suggested that the degree of decoupling between ionic conductivity and structural relaxation is fragility dependent: polymers with higher fragility index m exhibited a higher decoupling of σ_{dc} from the α-relaxation, which is consistent with other decoupling phenomena referred above. The phenomenological explanation given by Ngai's coupling model remains valid to explain the decoupling of ionic conductivity from structural relaxation.[69,75] In the framework of the CM the breakdown of the Stokes−Einstein and the Debye−Stokes−Einstein relationships are regarded as special cases of a more universal phenomenon that different dynamic observables (μ) weight the many-body relaxation differently and have different coupling parameters, $n_{\mu} = 1 - \beta_{KWW}$.[69,75] The temperature dependence of the Kohlrausch relaxation time, τ_{μ}, is given by the CM equation rewritten as $\tau_{\mu}(T) = [\tau_{0\mu}(T)t_c^{-n_{\mu}}]^{1/(1-n_{\mu})}$, where all primitive relaxations times, $\tau_{0\mu}$, have the same temperature dependence. Therefore, the relaxation time of the dynamical variable having the larger coupling parameter (smaller $\beta_{KWW} = 1 - n_{\mu}$) will show a stronger temperature dependence. This explanation is valid whether the coupling parameters are temperature dependent or independent.

Also worth mentioning are the works of Anderson, Johari, and coauthors where a detailed discussion of the effects that may be at the origin of observed deviations from the Debye−Stokes−Einstein ($\sigma_{dc} - \tau$) relationship has been given.[31,32,76] In addition, the importance of studies on the dc conduction phenomenon for the understanding of osmosis in biological processes and trans-dermal drug delivery was highlighted by those authors, who have reported studies on the influence of temperature and pressure on dc conductivity and relaxation time in an ultraviscous acetaminophen−aspirin mixture.[31,32]

Molecular mobility of the amorphous forms is generally recognized to be a key parameter governing the physical stability. However, it should also be noted that other factors may be expected to have some contribution to the physical stability.[77,78] Overall crystallization is a complex phenomenon usually interpreted in terms of processes of nucleation and growth that are affected differently by temperature. The occurrence of crystallization requires the formation of stable nuclei with a critical size on which the crystals will subsequently grow. For a variety of materials, the nucleation rate has a maximum above T_g, whereas the maximum growth rate is further displaced to higher temperatures between T_g and T_m.[43,79−81] The rate of nucleation and growth of the clusters of the newly evolving crystalline phase is dictated by (i) the rate of the diffusion of the molecules/ions that build up the crystalline phase, (ii) the driving force, the difference of Gibbs free energy between the crystalline and liquid states, and (iii) the interfacial free energy.[43,82,83] The roles of thermodynamic (as configurational entropy, enthalpy, or Gibbs free energy), molecular (as hydrogen bonding interactions), and kinetic (molecular mobility) factors and implication of the processing conditions, for the crystallization of drugs from the amorphous state were examined in a review by Bhugra and Pikal[77] and recently overviewed in detail by Laitinen et al.[78]

In the present work, dielectric relaxation spectroscopy (10^{-1} to 10^{6} Hz) is applied to obtain relevant information regarding the different molecular motions from the glass to the liquid state of *S*-flurbiprofen (from 173 to 408 K). Its chemical structure is shown in Figure 1.

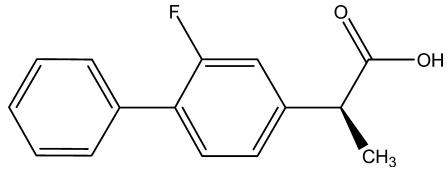

Figure 1. Chemical structure of *S*-flurbiprofen (*S*-(+)-[2-(3-fluoro-4-phenyl)phenyl]propanoic acid). The fluorine center and the oxygen of the carbonyl group can act as hydrogen bonding acceptor (HB), whereas the oxygen site of OH may acts both as HB acceptor and donor.

Flurbiprofen ((*R*,*S*)-[2-(3-fluoro-4-phenyl) phenyl] propanoic acid) is one of the most widespread nonsteroidal anti-inflammatory drugs (NSAIDs), used in the treatment of rheumatoid arthritis, osteoarthritis, mild to moderate pain and inflammatory diseases, particularly at the ophthalmic level.[84] It is usually administered in the racemic form; the *S*-enantiomer exhibits most of its anti-inflammatory activity.

Flurbiprofen belongs to the chemical class of NSAIDs commonly referred to as the "profens", related to ibuprofen ((2*R*,*S*)-2[4-(2-methylpropyl)phenyl]propanoic acid) in structure. Previous investigations on the structure and dynamics in the supercooled and glassy states of ibuprofen were carried out by some of us.[27] It was shown that in many aspects ibuprofen follows the typical behavior of nonpharmaceutical glass formers. Multiple relaxation processes were identified: the main α-relaxation associated with the dynamic glass transition, a β_{JG} Johari−Goldstein process taken as the precursor of the α-relaxation and a more localized secondary γ-relaxation. Moreover, in the supercooled liquid state ($T > T_g$), an additional relaxation process with a Debye-like shape (D-process) was observed at the low frequency side of the α-process, and it was assigned to peculiarities related to the dynamics of hydrogen-bonded aggregates.

In the present study, it is shown that the properties of *S*-flurbiprofen are generally similar to that of ibuprofen. It is aimed to give a further contribution to a better understanding of the molecular mobilities, which can cause changes during processing or even storage and handling of pharmaceutical substances. In addition to dielectric characterization, both standard and temperature modulated DSC (TMDSC) are applied for the thermal characterization of *S*-flurbiprofen.

2. EXPERIMENTAL SECTION

2.1. Material and Sample Characterization. *S*-Flurbiprofen (CAS-No. 51543-39-6), $C_{15}H_{13}FO_2$, molar mass of 244.261 g·mol^{-1}, was purchased from Aldrich (product number 482641−500 mg, lot number 18519 KB, purity ≥98%). It was a white, crystalline powder (melting point 382−383 K), and it was used without further purification.

Acetanilide (*N*-phenylacetamide), CAS No. 103-84-4, used to perform temperature calibration of the dielectric measurements was purchased from Wagner and Munz GmbH (ChemPur, Ch.020612). The certified equilibrium melting temperature of acetanilide is 387.05 K.

2.1.1. Optical Activity. Measurements of the specific rotation $[\alpha]_D$ of a solution of 1.015g/100 mL of the as-received *S*-flurbiprofen in chloroform were performed at room temperature, by means of a AA-1000 Polarimeter (Optical activity LTD). The optical path length of the measurement cell was 5 cm. Specific rotation $[\alpha]_D$ was calculated using the standard equation $[\alpha]_D = 100\alpha/cd$, where α is the measured angle of optical rotation (in angular degrees), D denotes the wavelength employed, which corresponds to the sodium D line, c is the concentration of the compound in grams per 100 mL solution, and d is the optical path length in decimeters. The average of three measurements of the optical rotation angle (+0.229°) gives $[\alpha]_D$ = +45° in good agreement with the values reported in the literature ($[\alpha]_D$ (24 °C) = +43°, c = 1; $CHCl_3$ (Sigma Aldrich); $[\alpha]_D$ (22 °C) = +41.4°, c = 1; $CHCl_3$ (ref 6 cited in ref 84).

2.1.2. Thermogravimetric Analysis. The thermal stability of *S*-flurbiprofen was studied by thermogravimetric analysis (TGA). A sample of 4.692 mg was placed in an open platinum sample pan and the TGA measurements were carried out with a TGA 7 apparatus from Perkin-Elmer, at a heating rate of 5 K·min^{-1} under highly pure nitrogen atmosphere with a flow rate of 20 mL·min^{-1}. The temperature reading was calibrated using the Curie points of alumel and nickel standards, while the mass reading was calibrated using balance tare weights provided by Perkin-Elmer. TGA and derivative curves are shown in Figure 2. The main weight loss event observed is due to the thermal decomposition that starts at around 433 K and is complete at ∼533 K (weight loss ∼100%). Both TGA and derivative curves show that decomposition occurs in a single weight loss step. In order to avoid degradation in the calorimetric and dielectric studies, samples were heated to a maximum temperature of 408 K. Moreover, after the dielectric measurements, the purity of the sample was also checked by thin layer chromatography using Merck silica gel 60 F254 plates: a single spot was visible perfectly identical to the reference spot obtained for the as-received *S*-flurbiprofen, confirming that no chemical degradation occurred during the thermal cycles to which the sample was subjected.

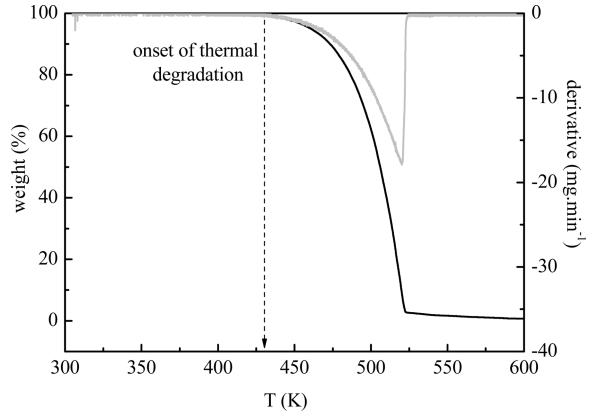

Figure 2. Thermogravimetric (black line) and derivative (gray thicker line) curves obtained on heating at 5 K·min^{-1} of the as-received crystalline *S*-flurbiprofen. The onset of thermal decomposition is indicated by the arrow (∼433 K). No weight loss is observed prior to this temperature also confirming the anhydrous characteristics of the as-received sample.

2.2. Experimental Techniques. *2.2.1. Differential Scanning Calorimetry.* Differential scanning calorimetry experiments were carried out with a 2920 MDSC system from TA Instruments Inc. interfaced with a liquid nitrogen cooling accessory (LNCA). Samples of sizes 4−6 mg were placed in aluminum pans and hermetically sealed using an encapsulating press. An empty aluminum pan, identical to that used for the sample, was used as reference. The measuring cell was continuously purged with high purity helium gas (at a flow rate of 30 mL·min^{-1}) to improve the thermal conductivity. The DSC runs cover a temperature range from 223 to 408 K using a heating/cooling rate of 10 K·min^{-1}. The baseline was calibrated scanning the temperature (from 193 to 453 K) on heating at 10 K·min^{-1} with two empty pans.

The temperature calibration was performed by taking the onset of the endothermic melting peak of a sample of indium supplied by TA Instruments Inc. (certified equilibrium melting temperature, 429.75 K); the enthalpy was calibrated by taking the peak area of the melting peak of indium (certified melting enthalpy 28.7100 J·g^{-1}). The calibration with indium was performed at the same heating rate, with the same type of pan and the same environmental conditions as in the experiments.

Additional temperature modulated DSC (TMDSC) experiments were carried out in the "heat-only" modulation mode (oscillation period of 60 s, amplitude of ±0.08 K), from 223 to 403 K at a heating rate of 0.5 K·min^{-1}. Heat capacity calibration was performed using a sapphire disk. The modulation scanning was performed on an initially amorphous sample obtained during a previous temperature cycle carried out on the conventional mode.

2.2.2. Dielectric Relaxation Spectroscopy. The complex dielectric function $\varepsilon^*(f) = \varepsilon'(f) - i\varepsilon''(f)$ (f, frequency; ε', real part; ε'', imaginary part) associated with reorientational motions of dipoles was measured by an Alpha-N impedance analyzer from Novocontrol Technologies GmbH, covering a frequency range from 10^{-1} Hz to 1 MHz. Approximately 12 mg of the as-received *S*-flurbiprofen crystalline powder was slightly compressed between two gold plated electrodes (upper electrode 10 mm diameter) of a parallel plate capacitor, with two silica spacers of 50 μm thickness (more details are given below in Temperature Calibration). The silica spacers were used in order to avoid contact between the disposable electrodes when the crystalline sample melts and to ensure, on the following measurements, a constant distance between the two electrodes, i.e., constant sample geometry (capacitance of empty capacitor C_0 = 13.91 pF). The sample capacitor was inserted in BDS 1200 sample holder, mounted on a cryostat, BDS 1100, and exposed to a heated nitrogen gas stream being evaporated from a liquid nitrogen Dewar. The temperature of the sample was controlled by a Quatro Cryo-system with temperature stability better than 0.5 K. Novocontrol GmbH supplied all these modules. After the first temperature scanning leading to melt, the contact between all elements was checked,

dx.doi.org/10.1021/mp4002188 | *Mol. Pharmaceutics* 2014, 11, 112−130

and if necessary, the top electrode of the sample holder was screwed again allowing fixing the sample thickness to 50 μm.

Dielectric measurements were carried out in both a temperature scanning mode (isochronal mode) and in an isothermal mode. In order to study the thermal transitions of *S*-flurbiprofen, the complex dielectric permittivity was measured in the isochronal mode, $\varepsilon^*(T)$, at five frequencies sufficiently high to allow a reliable measurement (10^2, 10^3, 10^4, 10^5, and 10^6 Hz) during heating/cooling cycles performed at a rate set to 10 K·min^{-1}, in the temperature range between 250 and 408 K.

In order to investigate the molecular mobility in the glassy state, supercooled and liquid state, the sample was kept 10 min at 408 K, slightly above $T_m \approx 384$ K, to ensure complete melting. The molten sample was cooled down to 173 K at ~10 K·min^{-1}, and the dielectric spectra were collected isothermally from T = 173 K to T = 408 K, increasing the temperature in different steps: in the range 173 K $\leq T \leq$ 263 K in steps of 5 K; from 263 to 353 K in steps of 2 K; and in the remaining temperature range in steps of 5 K. The maximum deviation from a set temperature was found to be ±0.2 K.

2.2.2.1. Temperature Calibration. For comparison of information about thermal transitions obtained by dielectric spectroscopy with that obtained by DSC it is necessary to calibrate the DSC temperature scale for the measuring conditions used, as well as to calibrate the dielectric spectrometer. However, implementation of temperature calibration strategies in dielectric measurements is not as straightforward as in DSC, and it is almost nonexistent.[85−87] It is usually considered that the sample's temperature is the one read by the thermocouple.[87] This approach can be considered reasonable for isothermal dielectric measurements, although thermal gradients might exist between the sample and the temperature sensor even at constant sensor temperature.[87]

In the Novocontrol GmbH measuring equipment used in the present study, the actual temperature process value of the sample is measured by a Pt-100 Ω sensor. The input for the Pt-100 sensor is calibrated by Novocontrol using precision resistors, which are specified to conform to DIN EN 60751. In spite of the fact that the temperature sensor is incorporated in the lower electrode of the sample holder, differences between sample and sensor temperatures may exist when performing dielectric experiments at nonisothermal conditions, i.e., dielectric measurements at some specified frequencies during temperature scans (isochronal experiments). As in many thermal analysis techniques, this thermal lag between the sample temperature and the sensor temperature will be most important for higher temperature rates (for the same sample mass).

Three different methods were suggested by Mano et al. and Dionísio et al.[86,87] to correct the temperature axis of isochronal dielectric experiments based on the detection of a relaxation or transition that is well characterized in terms of its position in the temperature axis. One method is based on the use of high purity metallic standards (like indium and tin).[85−87] The melting of the metal decreases the distance between the capacitor plates, and the capacitance (C) increases; the step observed in the measured capacitance allows the temperature calibration of dielectric experiments similar to the DSC:[85] in an equivalent way ε' can be used for temperature calibration[86,87] given that $\varepsilon' = C/C_0$, with C_0 being the capacitance of the empty capacitor. The melting temperature measured by the temperature sensor is compared with the exact one allowing the correction of the temperature. However such metallic materials cannot be used directly in dielectric experiments due to their high electrical conductivity. The proposed setup for temperature calibration comprises the use of metallic standards placed between two films of an insulating material.[85−87] Since this setup is very different from the sample geometry used in the present work to perform the dielectric characterization of *S*-flurbiprofen, an organic melting point standard, acetanilide, was used to check the temperature calibration of the dielectric measurements.

The calibration with acetanilide was carried out at the same heating rate, with the same type of sample geometry and the same environmental conditions as those in the isochronal experiments of *S*-flurbiprofen. Aproximately 10 mg of acetanilide crystalline powder was placed between two disposable gold plated electrodes (lower electrode 20 mm and upper electrode 10 mm diameter) with two silica spacers of 50 μm thickness (capacitance of the empty capacitor C_0 = 13.91 pF). The use of a lower electrode with 20 mm diameter intends to prevent that powder sample possibly in excess to flow outside of the capacitor upon melting, which would lead to scattered readings. This assembly was mounted in the BDS 1200 sample holder between two electrodes. The mobile top electrode was moved down until some pressure was created in order to ensure a good physical contact through all elements.[86] It was then fixed allowing maintaining the distance between the electrodes during the experiment. The silica spacers were used in order to avoid contact between the disposable electrodes when the crystalline sample melts.

Isochronal dielectric measurements (at 10^2, 10^3, 10^4, 10^5, and 10^6 Hz) were carried out scanning the temperature at a heating rate set to 10 K·min^{-1}, from room temperature to 403 K. The starting temperature was set well below the melting temperature to ensure the stabilization of the heating rate before melting.

Figure 3 shows the temperature dependence of the real part of dielectric permittivity, ε', of acetanilide measured at 9.6 K·min^{-1} (real heating rate) and at a frequency of 10^3 Hz. The temperature axis is the temperature read by the Pt-100 Ω

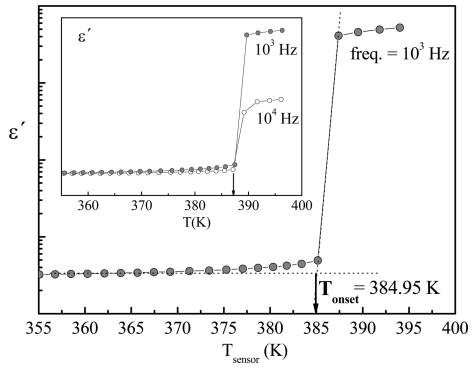

Figure 3. Temperature dependence of the real part of dielectric permittivity, ε', using acetanilide as standard, recorded at real heating rate 9.6 K·min^{-1} (target heating rate of 10 K·min^{-1}) and measured at 10^3 Hz. Absolute values for ε' are omitted due to the fact that both thickness and volume of the sample changes upon melting. The temperature axis, T_{sensor}, is the temperature given by the Pt-100 Ω sensor. The method for obtaining the onset temperature, T_{onset}, is shown. The certified equilibrium melting temperature of acetanilide is T_{th} = 387.05 K. Inset: $\varepsilon'(T)$ at two frequencies as a function of the sample temperature (after temperature correction).

dx.doi.org/10.1021/mp4002188 | *Mol. Pharmaceutics* 2014, 11, 112−130

sensor. Figure 3 illustrates the method for obtaining the onset melting temperature: the obtained onset temperature is 384.95 K, which is 2.1 K below the certified equilibrium melting temperature T_{th} = 387.05 K.

The inset shows the $\varepsilon'(T)$ trace obtained at two frequencies, where T is the correct sample temperature: the onset temperature is independent of the frequency used. This is the expected behavior given that melting is a first order thermodynamic transition. The use of $\varepsilon'(T)$ trace is preferred to the $\varepsilon''(T)$ trace since the latter is most frequently influenced by conductivity at high temperatures when sample starts to melt. The melting endothermic peak of acetanilide detected in the correspondent DSC thermogram (not shown) presents an extrapolated onset temperature $T_{m,onset}$ = 386.93 K. The temperature calibration allows obtaining a difference between the temperature scales of the DSC and the dielectric equipment less than 0.5 K for the heating rate used.

In order to check the temperature read for isothermal measurements, the complex dielectric permittivity of acetanilide was measured over frequency scans and as function of time while increasing the temperature to a set point temperature 387.15 K. These measurements were carried out using the same conditions for temperature stabilization as in isothermal measurements. The temperature read by the sensor was 386.89 K when acetanilide melts (T_{th} = 387.05 K). Therefore, in isothermal dielectric measurements, no temperature correction was done, and the sample's temperature is the one read by the Pt-100 Ω sensor.

2.2.2.2. Data Analysis. To analyze the isothermal dielectric data, the model function introduced by Havriliak–Negami[88] was fitted to both imaginary and real components of complex permittivity. Because multiple peaks are observed in the available frequency window, a sum of HN model functions was employed:

$$\varepsilon^*(\omega) = \varepsilon_\infty + \sum_k \frac{\Delta\varepsilon_k}{[1 + (i\omega\tau_{HN_k})^{\alpha_{HN_k}}]^{\beta_{HN_k}}} \quad (8)$$

where k sums over the different relaxation processes, ω is the angular frequency $\omega = 2\pi f$, τ_{HN} is a characteristic relaxation time that is related to the frequency of maximal loss f_{max}, $\Delta\varepsilon$ is the dielectric relaxation strength of the process under investigation, and ε_∞ is the high frequency limit of the real part $\varepsilon'(\omega)$; α_{HN} and β_{HN} are fractional shape parameters ($0 < \alpha_{HN} \leq 1$ and $0 < \alpha_{HN}\beta_{HN} \leq 1$) describing the symmetric and asymmetric broadening of the dielectric spectrum.

From the estimated values of τ_{HN}, α_{HN}, and β_{HN} parameters, a model-independent relaxation time, $\tau = (2\pi f_{max})^{-1}$, was calculated according to[89]

$$\tau = \tau_{HN} \times \left[\frac{\sin\left(\frac{\alpha_{HN}\beta_{HN}\pi}{2 + 2\beta_{HN}}\right)}{\sin\left(\frac{\alpha_{HN}\pi}{2 + 2\beta_{HN}}\right)} \right]^{1/a_{HN}} \quad (9)$$

Low frequency conductivity effects were taken into account for temperatures higher than 277 K by adding a contribution $(\sigma_{dc}/(\varepsilon_0\omega))$ to the imaginary part of the fitting function; σ_{dc} is the dc conductivity (pure Ohmic conduction) of the sample, and ε_0 is the vacuum dielectric permittivity. The complex conductivity contribution $\sigma^*(\omega) = \sigma'(\omega) + i\sigma''(\omega)$ is related to $\varepsilon^*(\omega)$ by $\sigma^*(\omega) = i\omega\varepsilon_0\varepsilon^*(\omega)$.[90]

3. RESULTS AND DISCUSSION

3.1. Differential Scanning Calorimetry. Differential scanning calorimetry experiments (conventional mode) and dielectric relaxation measurements (in the isochronal mode) were carried out in order to establish the conditions to obtain *S*-flurbiprofen in the amorphous form. Figure 4 shows the conventional DSC data collected during three successive temperature scans at a cooling/heating rate of 10 K·min^{-1}.

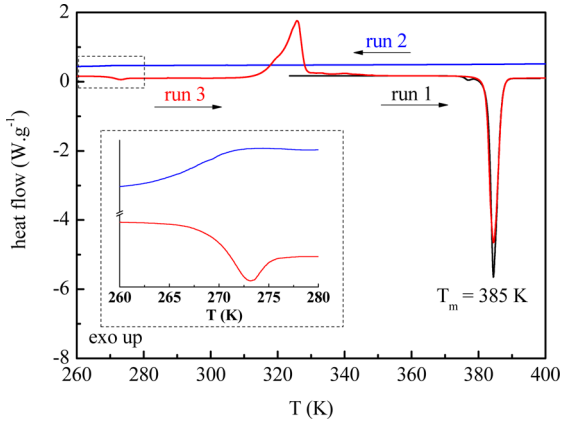

Figure 4. DSC thermograms of *S*-flurbiprofen obtained at heating/cooling rate of 10 K·min^{-1}. Run 1 (black line): heating of the as-received crystal (T_m = 384.5 K is the melting temperature taken at the peak). Run 2 (blue line): subsequent cooling from the molten state after a 10 min isothermal at 408 K. Run 3 (red line): subsequent heating to 408 K. The inset is a scale up of the glass transition region obtained on cooling (upper curve)/heating (lower curve) evidencing the heat flow jump. At higher temperatures an exothermic peak centered at 325.8 K is followed by a melting endotherm peak at 384.6 K.

In the first heating scan (run 1), the as-received crystalline *S*-flurbiprofen was heated from room temperature up to 408 K. A sharp endothermic peak (width at half height of 2.3 K) is observed: the melting transition has an extrapolated onset temperature at 382.8 K, peak temperature, T_m = 384.5 K, and an estimated enthalpy of melting, ΔH_m = 23 kJ·mol^{-1}. A small endothermic peak is observed immediately before the main endothermic response in the DSC heating scans of the material as-received; it is never seen in the second heating cycle (run 3 below), when the sample recrystallizes from the amorphous form. This thermal response that becomes less pronounced when the DSC experiment is carried out at heating rates <10 K·min^{-1} (not shown) is most probably due to a distribution of crystal sizes in the as-received material.

In the next cooling scan (run 2), crystallization is avoided (no exothermic peak is observed near below T_m), i.e., the system is supercooling, and upon further cooling it vitrifies at around 270 K (see scale up in the inset).

The subsequent heating scan from the glassy state (run 3) shows the characteristic signature for the glass transformation in the heat flow characterized by an onset temperature at $T_{g,onset}$ = 269.0 K, along with the typical enthalpy recovery peak (or endothermic overshoot); this T_g value agrees well with the one reported by Paradkar et al. (T_g = 268.5 K).[91] The heat capacity change between the glass and the supercooled liquid at T_g is ΔC_p = 90 J·(mol·K)$^{-1}$. At higher temperatures, between 303 and 351 K, an exothermic peak characteristic of a crystallization process emerges. It is followed by a sharp endothermic peak at

dx.doi.org/10.1021/mp4002188 | Mol. Pharmaceutics 2014, 11, 112–130

T_m = 384.6 K characterized by an enthalpy of 23 kJ·mol^{-1}. While melting is a thermodynamic process occurring at a fixed small range on heating slowly, crystallization is a kinetic process being set by the experimental conditions (heating rate, sample mass, cell geometry, etc.) at all temperatures below and above T_g. The values of the temperature (and enthalpy) of melting are similar to those obtained during the first heating scan (run 1) for the as-received *S*-flurbiprofen, which indicates that, when the glass is heated up beyond the T_g, crystallization occurred leading to the same crystalline form as the original one. Moreover, the area measured in the thermogram from a temperature just above the glass transition to 396 K is negligibly small (∼0.8 kJ·mol^{-1}) meaning that after the previous cooling at 10 K·min^{-1} the sample is almost fully amorphous before the glass transition.

The maximum of the crystallization exotherm is at T_{cr} = 325.8 K. The crystallization enthalpy decreases with undercooling below the melting point, $T_m - T_{cr}$, and is always lower than the melting enthalpy.[92,93] Assuming that the heat capacity difference between the amorphous and crystalline phases is constant in the temperature range between T_{cr} and T_m, the crystallization enthalpy at temperature T_{cr} can be written as

$$\Delta H_{cr}(T_{cr}) \approx \Delta H_m(T_{cr}) = \Delta H_m(T_m) - (T_m - T_{cr})\Delta C_p \quad (10)$$

where T_m and T_{cr} are, respectively, the equilibrium melting temperature and crystallization temperature, $\Delta H_m(T_{cr})$ is the enthalpy of melting of the purely crystalline state at the crystallization temperature, and ΔC_p is the C_p-jump corresponding to the glass transition. The fit of eq 10 to the experimental values gives $\Delta H_{cr}(T_{cr}) \approx \Delta H_m(T_{cr})$ = 18 kJ·mol^{-1} close to the value determined by the integration of the crystallization exotherm detected during the heating scan (19 kJ·mol^{-1}) meaning that almost complete crystallization was attained under the tested conditions.

Temperature modulated DSC on heating at 0.5 K·min^{-1} (heat-only modulation mode) was carried out in order to get further information about the dynamic glass transition and phase transformations of *S*-flurbiprofen. TMDSC allows deconvoluting the total heat flow signal, as measured in conventional DSC, in the heat capacity and kinetic components (usually referred as reversing and nonreversing components). For the latter, kinetic events such as crystallization and enthalpy recovering contribute, while the glass transition manifests as a heat capacity change.[94]

Figure 5a shows the TMDSC scan for glassy *S*-flurbiprofen (obtained by the melt quench/cooling method during a previous conventional DSC cycle). The analysis allowed to separate the glass transition from the kinetic signal, being identified in the reversing component ($T_{g,onset}$ = 265.6 K; ΔC_p = 85 J·(mol·K)$^{-1}$). In the kinetic (nonreversing) signal the enthalpy recovery (at ∼265 K) and the cold-crystallization peak are clearly seen. The recrystallization exotherm is observed in the nonreversing signal with an extrapolated onset temperature of 300.1 K (peak crystallization at T_{cr} = 305.5 K), and with a corresponding decrease in the heat capacity noted in the reversing heat flow component.

Figure 5b compares the conventional heat flow obtained at a heating rate of 10 K·min^{-1} with the total heat flow (TMDSC experiment at 0.5 K·min^{-1}) revealing the influence of the heating rate in the crystallization process. Since crystallization is a kinetically controlled event it is highly influenced by the time scale of the experiment set by the heating rate. The

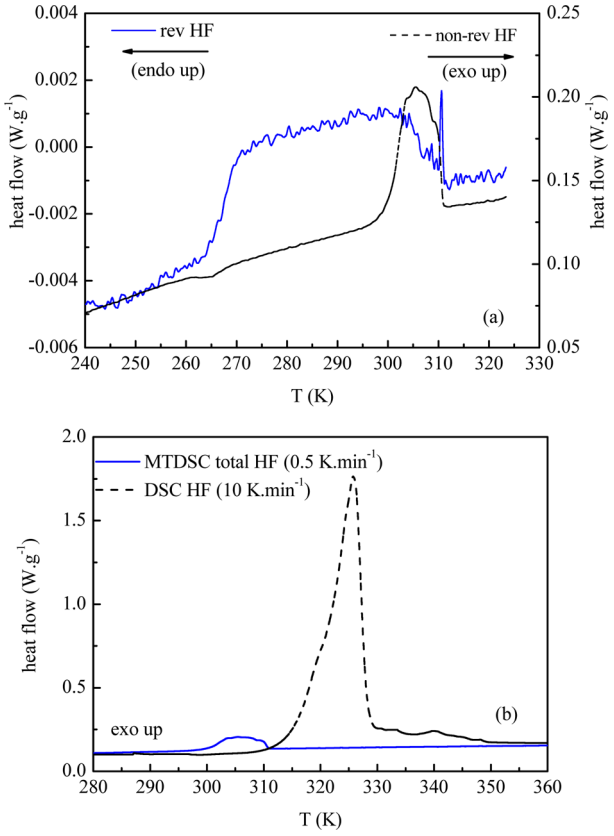

Figure 5. (a) TMDSC signals obtained on heating at 0.5 K·min^{-1} (heat-only modulation mode): kinetic component, i.e., nonreversing heat flow (black dashed line), and heat capacity component, i.e., reversing heat flow (blue solid line). (b) Comparison of the total heat flow signal (blue solid line) and conventional heat flow at 10 K·min^{-1} (black dashed line) in the temperature range where crystallization of *S*-flurbiprofen occurred.

recrystallization peak appears at lower temperatures and takes place over a narrower temperature range for the lower heating rate. The thermodynamic melting process (not shown) is observed at T_m = 383.04 K (peak temperature) with a melting enthalpy ΔH_m = 25.3 kJ·mol^{-1}. From eq 10 an estimated crystallization enthalpy of 18.7 kJ·mol^{-1} (≈ $\Delta H_m(T_{cr})$) is obtained in very good agreement with the value obtained from the integration of the recrystallization exothermic peak ($\Delta H_{cr}(T_{cr})$ = 18.8 kJ·mol^{-1}) validating the previous conclusions based on the analysis of the conventional DSC results.

3.2. Dielectric Relaxation Spectroscopy. *3.2.1. Isochronal Studies.* The temperature dependence of the real part of the complex dielectric permittivity, ε', is a valuable property to probe thermal transitions in low molecular weight compounds[95,96] including pharmaceutical drugs.[27,29] A thermal protocol similar to conventional DSC was performed, and the complex dielectric permittivity, $\varepsilon^*(T)$, in *S*-flurbiprofen was measured in isochronal mode at five frequencies.

Figure 6 presents the isochronal plots of both ε' and ε'' at three representative frequencies collected in successive runs at heating/cooling rate of ∼10 K·min^{-1}. The melting of *S*-flurbiprofen was monitored by measuring $\varepsilon^*(T)$ from room temperature up to 408 K (first heating run shown in Figure 6a): $\varepsilon'(T)$ shows a steep increase, which is a frequency-independent thermal event as expected for a first order thermodynamic transition. The onset temperature is T_{onset} = 382 K, and the end

dx.doi.org/10.1021/mp4002188 | *Mol. Pharmaceutics* 2014, 11, 112−130

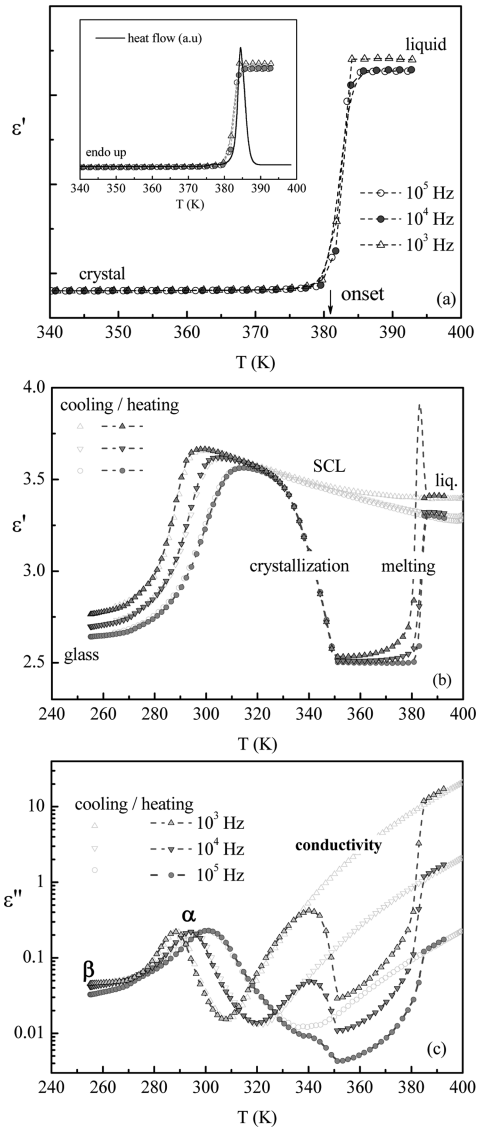

Figure 6. Temperature dependence of both real, ε', and imaginary, ε'', parts of the complex dielectric function for frequencies $f = 10^3$, 10^4, and 10^5 Hz collected in heating/cooling ramps at ~10 K·min^{-1}. (a) ε' trace obtained on heating of a slightly compressed powder of the as-received crystalline *S*-flurbiprofen. The observed steep increase of ε' is the melting transition at $T_m \approx 382$ K. The inset compares the ε' trace and the correspondent DSC obtained during heating at 10 K·min^{-1}; (b,c) $\varepsilon'(T)$ and $\varepsilon''(T)$, respectively, collected in following cooling (gray open symbols) and heating (filled symbols) ramps. On cooling, ε' and ε'' traces evidence the bypass of crystallization and further occurrence of the dynamic glass transition (α-relaxation). On heating, the frequency independent drop in the ε' trace (and ε'' trace) that ends at 350 K indicates that cold-crystallization occurred followed by melting at $T_m \approx 382$ K. Lines are guides for the eyes.

point temperature is 384 K. Both temperatures are in very good agreement with the onset and midpoint of the melting endothermic peak detected in the correspondent DSC heating thermogram, respectively, $T_{onset,DSC}$ = 382.8 K and $T_{m,peak}$ = 384.5 K. Absolute values for ε' are omitted due to the fact that both thickness and volume of the sample changes during melting (see details in section 2.2.2).

During subsequent cooling (light gray open symbols, Figure 6b), after the sample being kept at 408 K for 10 min in order to ensure complete melting, no discontinuity occurs around T_m, which indicates that crystallization does not take place and a supercooled liquid (SCL) is obtained, in agreement with the DSC results. $\varepsilon'(T)$ linearly increases with temperature decrease down to around 315 K followed by a frequency dependent step decrease indicating the transformation from the supercooled liquid to the glass; in the ε'' trace (light gray open symbols, Figure 6c), this corresponds to a frequency-dependent relaxation peak, i.e., the α-relaxation process associated with the dynamic glass transition. At the lowest temperatures, a broad and low intense peak is observed in the glassy state, the secondary β-relaxation related to localized molecular motions. At the highest temperatures, ε'' increases as temperature increases due to conductivity effects. The detailed dielectric study of the different relaxation processes and conductivity will be discussed later in the text.

Upon the subsequent heating scan (filled symbols, Figure 6b), after the characteristic signature for the glass softening, the sample undergoes cold-crystallization, which is visible in the plot just above 320 K by a decrease in $\varepsilon'(T)$. This is a frequency-independent event as expected for a thermodynamic first-order process; the drop in ε' ends at 350 K reaching a plateau value of ~2.5 typical of a crystalline phase. Note that this value is slightly lower than the permittivity of the glass (below T_g) because the latter secondary relaxations contribute (Figure 6c).

Crystallization leads also to a drop in the ε'' trace (filled symbols, Figure 6c), which is visible in the conductivity tail between 340 and 350 K. The temperature where crystallization starts is not exactly the same if probed by the drop in ε' (sensitive to dipolar relaxations but not influenced by conductivity) or by the decrease in the ε'' trace. Since both ε' and ε'' traces are measured simultaneously with the same heating rate and same frequency, this behavior results from the different time scales of the dipolar molecular motions (relaxation contribution) and of the ionic translational motions that are in the origin of conductivity tail reflecting the kinetic character of the crystallization process. These results nicely show that the measurement of the complex dielectric permittivity in a temperature scanning mode (isochronal experiments) is a very suitable tool to monitor phase transitions allowing detection in the same scan as the thermodynamic and kinetic character of the underlying processes.

The further increase in both real and imaginary parts observed near 382 K is due to the melting of the crystalline phase thus formed; the ε' and ε'' values superimpose those of the equilibrium liquid at a temperature around 384 K, i.e., the cold-crystallized sample melts at the same temperature as the as-received crystal, in very good agreement with the DSC results. Again, it can be concluded that the crystalline form thus obtained is the same as the original one. Both techniques DSC and DRS show that amorphous *S*-flurbiprofen is not stable upon heating.

The present results show once more that ε' is a valuable property to probe melting and crystallization transitions, with the advantage of being frequency independent and not affected neither by conductivity nor implying any data modeling. Another interesting advantage afforded by the analysis of the $\varepsilon'(T)$ data is that it allows also obtaining some structural information without any data modeling (gray open symbols in Figure 6b). Considering the polar carboxylic moiety, the fluorine atom (see structure in Figure 1), and the dipole moment of 2.35 D found for an isolated molecule (B3LYP/6-31G*), the liquid's equilibrium dielectric permittivity is rather

dx.doi.org/10.1021/mp4002188 | *Mol. Pharmaceutics* 2014, 11, 112−130

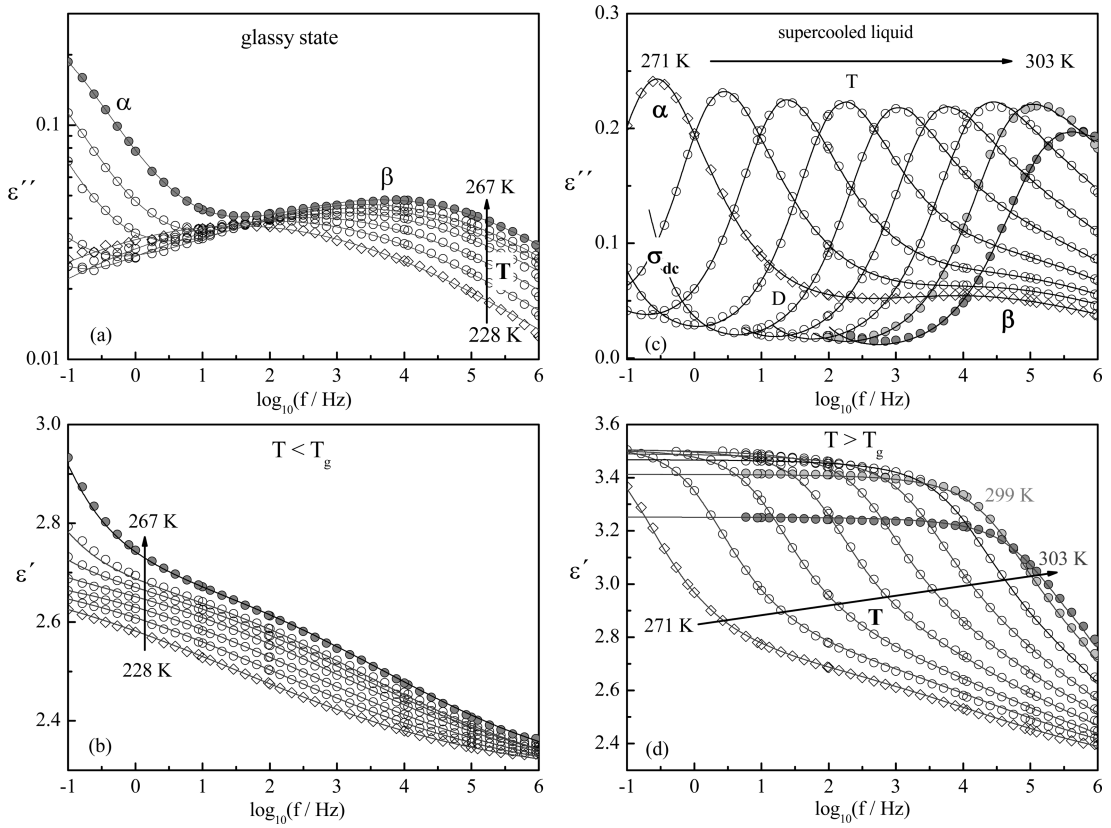

Figure 7. Imaginary (ε'') and real (ε') part of the dielectric permittivity versus frequency of amorphous *S*-flurbiprofen: (a,b) in the glassy state, from 228 to 263 K, in steps of 10 K, and 265 and 267 K; (c,d) in the supercooled liquid state, from 271 to 303 K, in steps of 4 K. Solid lines are the overall HN fitting curves to data. For clarity reasons, at temperatures higher than 287 K, when the conductivity contribution becomes important, data and fitting curves have been suppressed from the lower frequency part of the spectra.

low, ~3.5 (order of magnitude found for nondipolar liquids). It is an indication that hydrogen-bonding in *S*-flurbiprofen favors an antiparallel correlation of the dipole vectors.

The increase in the ε' trace obtained upon cooling from the liquid is related to the expected increase of the dielectric strength, $\Delta\varepsilon = \varepsilon_s - \varepsilon_\infty$; ε_s and ε_∞ are the limits of the real part of the dielectric permittivity at low and high frequencies, respectively, the latter being approximately the permittivity of the glass.[97] The starting point for the analysis of $\Delta\varepsilon$ is the extension of the Debye theory by Onsager, Fröhlich, and Kirkwood:[98]

$$\Delta\varepsilon = \frac{1}{3\varepsilon_0} g_K F \frac{\mu_0^2}{k_B T} \frac{N}{V} \qquad (11)$$

where ε_0 is the vacuum permittivity, μ_0 the dipole moment of the moving unit in vacuum, $F \approx 1$ is the Onsager factor calculated in the frame of the reaction field, T the temperature, k_B the Boltzmann constant, and N/V the number density of dipoles. g_K is the Kirkwood correlation factor that takes into account short-range intermolecular interactions that lead to specific static dipole−dipole orientations. For predominantly parallel or antiparallel correlations between neighboring dipoles, $g_K > 1$ or $0 < g_K < 1$, respectively, while for a random orientation of dipoles $g_K = 1$ holds. High values of the dielectric strength are observed when $g_K > 1$, while low values correspond to $g_K < 1$.[23]

According to eq 11, when crystallization is avoided (i.e., no dipolar moment is lost due to immobilization that would occur if crystallization had taken place), the dielectric strength is proportional to $(g_K\mu_0^2)/(k_BT)$. Assuming that g_K is constant, an increase in $\Delta\varepsilon$ from 379.34 to 346.98 K of 8.5% is predicted. Nevertheless, the observed raise taken into account in the permittivity data shown in Figure 6b is only 3.6% (ε'_{379K} = 3.32; ε'_{347K} = 3.44). As mentioned previously, the absence of discontinuity in the ε' trace when temperature decreases until the region where the α-relaxation evolves, probes that crystallization of *S*-flurbiprofen was circumvented upon cooling from the molten state. The fact that the observed variation of dielectric strength is smaller than that predicted by the Onsager−Fröhlich−Kirkwood equation indicates that during cooling of the liquid there is an enhancement of the antiparallel correlation (g_K decreases, and consequently, the effective dipole moment decreases) with temperature decrease. An even more important discrepancy was observed for ibuprofen: $\Delta\varepsilon_{predicted}$ = 8.5%, while $\Delta\varepsilon_{real}$ = 0.1% (calculus based on data shown in Figure 7 of ref 27). In fact, for ibuprofen it was shown that the distribution of hydrogen-bonding aggregates changes with temperature in such a way that on decreasing temperature the antiparallel correlation is enhanced, i.e. the Kirkwood correlation factor, $g_K < 1$, decreases: the antiparallel alignment of cyclic aggregates is increasingly more favorable with temperature decrease and partially compensates the increase predicted by the Onsager−Fröhlich−Kirkwood equation (eq 11). Thus, the low values of dielectric permittivity (and $\Delta\varepsilon$ as well) here reported are an indication that hydrogen-bonding in *S*-flurbiprofen, like in ibuprofen, favors an antiparallel correlation of the dipole vectors ($g_K < 1$).[23,27]

dx.doi.org/10.1021/mp4002188 | *Mol. Pharmaceutics* 2014, 11, 112−130

3.2.2. DRS Isothermal Studies. 3.2.2.1. Characterization of Molecular Mobility of Amorphous S-Flurbiprofen. An amorphous sample of *S*-flurbiprofen obtained by previous cooling of the liquid at ~10 K·min^{-1} was studied by DRS by performing a set of isothermal frequency sweeps on heating from 173 to 408 K (see experimental section).

Figure 7 shows illustrative dielectric spectra acquired in the available frequency range covering a wide temperature interval from the glass to the supercooled state. Parts a and c of Figure 7 show the dielectric loss spectra (ε'') and parts b and d present the dielectric permittivity spectra (ε'). Multiple relaxation processes take place in *S*-flurbiprofen. In the glassy state, at the lowest temperatures, a low intensity but well-defined broad secondary process is observed, here designated as β-relaxation (Figure 7a,b). In the supercooled liquid state, the β-process becomes submerged under the main relaxation process (α-relaxation) associated with the dynamic glass transition (Figure 7c). At higher temperatures (>301 K), a decrease in both real and imaginary parts of the complex permittivity is observed with the consequent decline of the dielectric strength of the α- and β-processes that become completely extinguished above 311 K (data not shown).

It is worth commenting that in the temperature range from 263 to 353 K, where isothermal dielectric spectra were acquired in steps of 2 K, an average heating rate of around 0.4 K·min^{-1} is obtained close to the average heating rate in the TMDSC experiment (0.5 K·min^{-1}). Following this approach, the time scale (imposed by the thermal treatment) for both experiments is comparable, and recrystallization of the sample above T_g occurs over the same temperature range: Figure 8 shows the

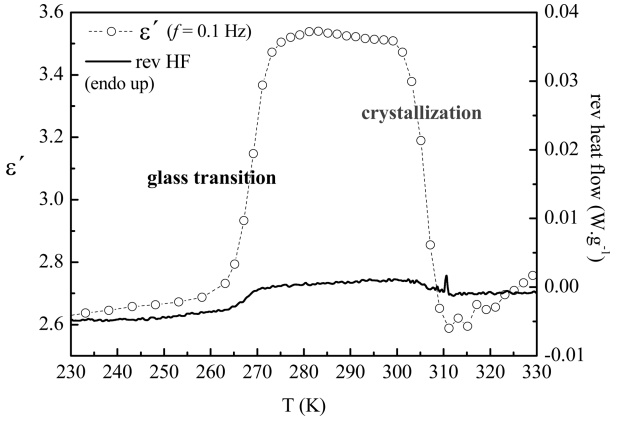

Figure 8. Comparison of the temperature evolution of the real part of the dielectric permittivity, $\varepsilon'(T)$ taken from isothermal data at a frequency f = 0.1 Hz (equivalent heating rate 0.4 K·min^{-1}) with the TMDSC reversing heat flow signal (heat capacity component) with a modulation of ±0.08 K over a 60 s period ($f \approx 0.02$ Hz) and heating rate of 0.5 K·min^{-1}.

temperature dependence of ε' at 0.1 Hz (taken from the isothermal dielectric data) in comparison with the reversing heat flow (the modulation period, 60 s, is equivalent to a frequency of 0.02 Hz). The decrease of ε' due to crystallization is frequency independent as typical for a first-order process (recalling Figure 6b) and corresponds to a step change in the heat capacity noted in the reversing heat flow component, which in turn reflects also the decrease in molecular mobility when the material crystallizes. As expected, the transformation to the crystalline phase takes place over a narrower temperature interval with a corresponding lower onset temperature as it was obtained from the dielectric isochronal measurements and conventional DSC as well.

The Havriliak–Negami function (eq 8) was fitted to the isothermal dielectric data shown in Figure 7 (both real and imaginary parts were analyzed) where additive behavior is assumed for taking into account the contribution of the two processes identified above. During the fitting procedure a third process (Debye-type) of weak intensity and located at frequencies between the conductivity tail and the α-relaxation was also considered; a detailed discussion of this process is out of the scope of the present study and it will be presented in detail elsewhere. The overall fitting curves are included in Figure 7. This fitting procedure allows extracting the spectral shape, the dielectric strength, and the mean relaxation time for each process, which are discussed in the following in detail.

Concerning the spectral shape, the β-relaxation shows a non-Debye behavior, as it is common for secondary relaxations. It is well described by a symmetrical Cole–Cole distribution function ($\beta_{HN,\beta} = 1$) with $\alpha_{HN,\beta} \approx (0.21–0.25)$ for temperatures below T_g and continuously increasing up to 0.49 in the temperature range above T_g.

The shape of the α-relaxation has a weak temperature dependence: $\alpha_{HN,\alpha} = 0.82 \pm 0.01$ and $\beta_{HN,\alpha} = 0.54 \pm 0.02$. The α-relaxation dispersion is well described by the one-sided Fourier transformation of the stretched exponential function KWW function (eq 3), $\varepsilon''(\omega) = \Delta\varepsilon \int_0^\infty (-d\phi/dt) \sin(\omega t)\, dt$, with a stretching parameter $\beta_{KWW} = 0.52$, which reflects the non-Debye nature of the relaxation response as it is usually observed in many supercooled liquids.[52] The estimated β_{KWW}-parameter will be later used for a quantitative discussion.

Figure 9 presents the temperature dependence of the model-independent relaxation times, τ (eq 9).

For temperatures below T_g, the relaxation time for the β-secondary process follows a linear temperature dependence of $\log(\tau)$ vs $1/T$ as it is characteristic of localized molecular mobility persisting in the glassy state. From the Arrhenius equation, $\tau(T) = \tau_\infty \exp(E_a/RT)$ (R (ideal gas constant) = 8.3145 J·mol^{-1}·K^{-1}), the values of the activation energy E_a = 52.5 kJ·mol^{-1}, and the pre-exponential factor $\tau_\infty = 3.93 \times 10^{-15}$ s were estimated. They are typical of noncooperative, local mobility. Around T_g the temperature dependence of the relaxation time of the β-process exhibits a strong change, i.e., the Arrhenius-like temperature dependence of τ_β below T_g cannot be extrapolated to temperatures above T_g. Note that for these temperatures, higher but close to T_g, the β-process remains well separated from the α-relaxation as seen in the ε'' raw data shown in Figure 7a allowing to obtain the τ_β and the dielectric strength, $\Delta\varepsilon_\beta$, from the HN fitting procedure. It should be noted that this procedure assumes that the α- and β-processes are additive, which may not be true. Consequently, the obtained τ_β and $\Delta\varepsilon_\beta$ should be considered as approximations to their actual values. The crossover of the τ_β(T) trace below the glass transition to stronger temperature dependence above T_g has also been observed directly in the raw data for different systems[45] including pharmaceuticals (e.g., ibuprofen[27] and telmisartan[38]). This behavior can be discussed in the framework of the coupling model that postulates a primitive relaxation process as a precursor of the α-relaxation, which is the analogue of the so-called Johari–Goldstein relaxation.[61−63] The relationship between the JG-process relaxation time, τ_{JG}, and the α-process, τ_α, is given by the CM equation (eq 5); using $\beta_{KWW} = 0.52$ (i.e., $n = 1 - \beta_{KWW} = 0.48$) and $t_c = 2 \times$

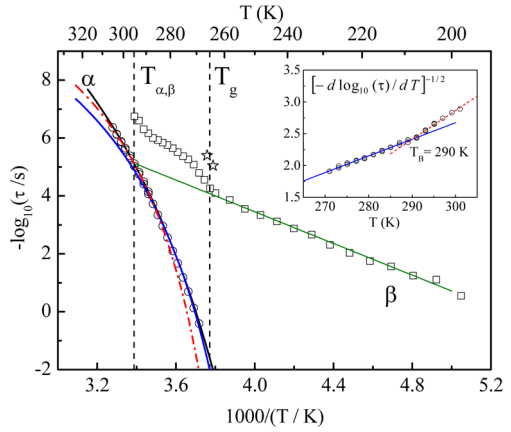

Figure 9. Relaxation time, τ, versus $1/T$ for the secondary β-relaxation (□) and for the main α-process (○). Lines are fits of the Arrhenius and VFTH formulas to the corresponding data: in the α-trace the black line is the VFTH fit to all temperature ranges, the blue line is the $VFTH_1$ fit, and the dashed (red) line is the $VFTH_2$ fit, respectively, to low and high-T data (see text and parameters in Table 1). Vertical dashed lines are the dielectric glass transition temperature T_g^{DRS} (τ = 100 s) = 265 K and the crossover temperature between the α-trace and the extrapolation of the Arrhenius low temperature dependence of β-relaxation, $T_{\alpha\beta}$ = 295.3 K. Stars indicate the JG relaxation time, $\tau_{JG} \approx \tau_0$, estimated from the CM (eq 5). Inset: Derivative plot, $[-\mathrm{d}\log_{10}(\tau)/\mathrm{d}T]^{-1/2}$ vs temperature, for the α-relaxation time. The solid blue line is a linear regression to the low-temperature data where $VFTH_1$ regime holds, while the dashed red line is the linear fit to the high temperature data characterized by $VFTH_2$. The intersection of the two lines defines the crossover temperature T_B = 290 K ($\sim T_{\alpha\beta}$) where $\tau \approx 10^{-4.2}$ s.

10^{-12} s, it gives a value of τ_{JG} at T_g of 6×10^{-6} s, which, within the experimental errors, is in good agreement with the experimental τ_β value at this temperature (stars in Figure 9). At T_g, there is a separation of about 6 decades between the α- and β-relaxation, i.e., the decoupling index defined as $d_\beta(T_g) = \log_{10}[\tau_\alpha(T_g)/\tau_\beta(T_g)] \approx 6$, as found in other molecular glass formers that show a well separate Johari–Goldstein β-process (d = 6–7 decades).[33] Another correlation usually associated with a JG β-process refers to the activation energy. Below T_g, the activation energy of the β-process estimated from the Arrhenius equation ($E_{a\beta}$ = 53 kJ·mol^{-1}) gives for the ratio $E_{a\beta}/RT_g$ a value of 24 matching the value proposed by Kudlik et al.,[99] $E_{a,JG} = 24RT_g$, that was found in genuine JG relaxation processes observed for several glass formers.[100] A further test to verify the nature of the β-relaxation is given by the relationship[100]

$$\frac{E_{a\beta}}{RT_g} = 2.303(2 - 13.7n - \log_{10}\tau_\infty) \quad (12)$$

which is equal to the CM equation and relates both Arrhenius parameters (activation energy $E_{a\beta}$ and prefactor τ_∞) of the secondary relaxation in the glassy state with the parameters of α-relaxation at T_g ($n(T_g)$, where T_g is defined by $\tau_\alpha(T_g)$ = 100 s); in *S*-flurbiprofen this relationship is well fulfilled: $((E_{a\beta})/(RT_g)) \approx 24$ and $2.303(2 - 13.7n - \log_{10}\tau_\infty) \approx 23$, which strengths the relationship between the structural α-relaxation and the secondary β-process. The change of τ_β at T_g, its correlation with τ_α, and the relationship of the activation energy of the β-process in the glassy state with T_g suggests that the detected β-relaxation in *S*-flurbiprofen is a genuine Johari–Goldstein process, attributed to a local motion of the molecule as a whole and regarded as the precursor of the structural α-relaxation.

An extra point that strengthens classification of the observed β-process as a JG-type comes from the analysis of the temperature dependence of the dielectric strength, $\Delta\varepsilon$, that is proportional to the amount of relaxing units. Figure 10 shows

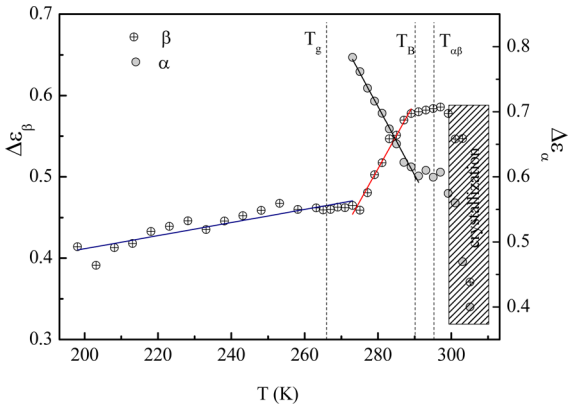

Figure 10. Dielectric strength, $\Delta\varepsilon$, versus temperature for the β-relaxation (left-hand axis; crossed circles) and the α-relaxation (right-hand axis; gray filled circles). The dashed area delimits the temperature range where crystallization occurs leading to a decreasing in the dielectric strength of both relaxations.

the temperature dependence of the dielectric strength for the β- and α-process detected in *S*-flurbiprofen: $\Delta\varepsilon_\beta$ increases with temperature increase. For a localized process like the β-relaxation, $\Delta\varepsilon_\beta$ generally increases with temperature due to an increase of the number of fluctuating dipoles and/or the fluctuation angle of the dipole vector with temperature[101,102] according to the Onsager–Fröhlich–Kirkwood relationship (eq 11). Interestingly, the increase of $\Delta\varepsilon_\beta$ with increasing temperature (Figure 10) becomes more prominent on crossing the glass transition; there is a crossover of the temperature dependence of $\Delta\varepsilon_\beta$ with an elbow shape. This kind of behavior was also found for other glass formers (e.g., D-sorbitol) and taken as a further indication of the connection between the JG β-process and the α-relaxation (see ref 45 for details and references therein): the observed change in the dielectric strength on heating through the glass transition mimics the changes observed for thermodynamic quantities like enthalpy, entropy, and specific volume.

Figure 10 shows also that, differently from the β-relaxation, the dielectric strength for the α-process, $\Delta\varepsilon_\alpha$, decreases with increasing temperature as it is well-known for conventional glass formers.[103] The temperature dependency of $\Delta\varepsilon_\alpha$ is stronger than predicted by eq 11, a recognized characteristic of the α-relaxation that can be explained by the cooperative character of the underlying molecular motions responsible for glassy dynamics.[104] Above 303 K, an abrupt drop is observed in the dielectric strength of both α- and β-relaxations attributed to crystallization of the sample on heating. We must note that the growing of crystal units of *S*-flurbiprofen, similarly to results found in other pharmaceutical drugs[36,105] and low molecular weight glass formers,[95,96,106] does not influence (data from isothermal crystallization is not shown here) the α-relaxation time, τ_α, that is now taken for analysis in the temperature range $T_g < T \leq 303$ K.

dx.doi.org/10.1021/mp4002188 | *Mol. Pharmaceutics* 2014, 11, 112–130

For the α-relaxation, the temperature dependence of the relaxation time is curved when plotted versus $1/T$ (Figure 9) being described by the empirical VFTH equation (eq 1). The estimated parameters for the α-relaxation of *S*-flurbiprofen are B = 2480 K, T_0 = 209 K, and $\tau_\infty = 10^{-18}$ s. Typically, in the high temperature limit the dielectric relaxation time and the pre-exponential factor, τ_∞, in eq 1, is about $\sim 10^{-14}$–10^{-13} s, describing local orientational fluctuations. Thus, the lower value found here (10^{-18} s) leads us to doubt the validity of the fitting. In fact, for many glass forming liquids, it has been found that a single VFTH-law describes the temperature dependence of the relaxation times only up to a characteristic temperature T_B, which is 10–50% higher than T_g.[44] At T_B, the temperature dependence of τ changes from a low temperature VFTH-behavior to a high temperature one. The origin of this dynamic crossover is not yet entirely understood. In the framework of the coupling model the dynamic crossover at T_B can be ascribed to the onset of significant increase of intermolecular cooperativity.[45,107,108]

For a detailed analysis of the temperature dependency of the α-relaxation, a derivative method is applied,[70,103,109−111] which is sensitive to the functional form of $\tau(T)$ irrespective of the pre-exponential factor. For a dependency of $\tau(T)$ according to the VFTH-equation (eq 1) one obtains

$$\left[\frac{\mathrm{d}\log_{10}(1/\tau)}{\mathrm{d}T}\right]^{-1/2} = \left(\frac{B}{2.303}\right)^{-1/2}(T - T_0) \tag{13}$$

Thus, the plot of $[(-\mathrm{d}\log_{10}(\tau))/(\mathrm{d}T)]^{-1/2}$ versus temperature linearizes the VFTH behavior evidencing the inadequacy of a single VFTH expression to fit the temperature dependence of τ_α. The change in dynamics at T_B can be observed for *S*-flurbiprofen in the inset of Figure 9: two VFTH equations (one at high, $VFTH_2$, and one at low temperatures, $VFTH_1$) have to be used to describe the data in the whole temperature range. These fits are shown respectively as solid blue ($VFTH_1$) and dashed ($VFTH_2$) red lines in the relaxation map (parameters in Table 1). The dielectric glass transition temperature calculated by extrapolation of the $VFTH_1$ fit to the relaxation time τ = 100 s is T_g^{DRS} = 265.2 ± 0.2 K, in excellent agreement with the value obtained from the TMDSC results, $T_{g,onset\ (TMDSC)}$ = 265.6 K. It must be noted that (i) the glassy state was obtained in both experiments by the melt/cooling method at the same set cooling rate (10 K·min^{-1}); (ii) the average scanning rate in the TMDSC experiment was 0.5 K·min^{-1}, very close to the average heating rate corresponding to the isothermal dielectric measurements in the glass transition region (0.4 K·min^{-1}). Both (i) and (ii) determine the thermal glass transition temperature; (iii) the TMDSC experiment was carried out with an oscillation period of 60 s corresponding to a relaxation time of ∼10 s that determines the time scale of the dynamic glass transition;[85] thus, when comparison is made at $T_g(\tau = 100\ \mathrm{s})$ the time scale of both experiments is very close and the obtained values of the glass transition temperature agree very well.

Table 1. Parameters of the VFTH Function (eq 1) Used to Describe the Temperature Dependence of the α-Relaxation Time; VFTH Parameters (eq 15) Used to Describe the T Dependence of dc Conductivity, σ_{dc}

	B (K)	τ_∞ (s)	T_0 (K)
VFTH (α) (all T range)	2480	2.3×10^{-18}	209
$VFTH_1$ (α) (low T range)	1228	9.1×10^{-14}	230
$VFTH_2$ (α) (high T range)	992	9.9×10^{-14}	241
	B_σ (K)	σ_∞ (S·cm^{-1})	$T_{0,\sigma}$ (K)
VFTH (σ_{dc})	1624	1.0×10^{-4}	215

The intersection of the two VFTH lines (inset of Figure 9) gives a crossover temperature T_B = 290.1 K. This temperature is close to the one estimated from extrapolating the β-trace ($\tau_\beta(T)$) obtained below T_g with the α-trace ($\tau_\alpha(T)$), $T_{\alpha\beta}$ = 295.3 K. In spite of the deviation observed from the Arrhenius temperature dependence of τ_β at T_g, this is the conventional way to estimate the merging of the two processes[112] occurring close to T_B for a variety of nonpharmaceutical glass formers.[113] To the best of our acknowledge, reports on this crossover at T_B are scarce in the pharmaceutical literature: examples are nicotine,[25] ibuprofen,[27] telmisartan,[38] and celecoxib.[30] In the latter study, the authors correlated the crystallization kinetics of amorphous celecoxib with the dynamics of the α-relaxation above T_B. For *S*-flurbiprofen, T_B ($\sim T_{\alpha\beta}$) is close to the temperature where cold-crystallization occurs during heating from the glassy state (recalling Figure 10). The connection between the observed crossover in the α-relaxation dynamics and crystallization of *S*-flurbiprofen will be discussed in a forthcoming publication.

Using the VFTH expression (eq 1) and eq 2, the fragility index m can be calculated according to

$$m = \frac{BT_g}{\ln 10(T_g - T_0)^2} \tag{14}$$

Taking the B and T_0 values of the $VFTH_1$ fit to the α-relaxation (Table 1), a fragility index of m = 113 ± 2 being estimated for *S*-flurbiprofen allows to classify it as a fragile glass former. The correlation between m and the stretched exponent β_{KWW}, proposed by Böhmer et al.[52] (eq 4), is reasonably verified for *S*-flurbiprofen: using β_{KWW} = 0.52, it gives m = 82.6 ± 30 (higher limit value 113.6 being identical to m obtained from eq 14). In spite of the broad application of Böhmer et al.'s empirical correlation between β_{KWW} and m, some exceptions exist such as the case of the anti-inflammatory drug celecoxib:[13] it is a fragile glass former (m = 110) and its α-loss peak being characterized by a small degree of nonexponentiality (β_{KWW} = 0.67). It was found that the amorphous celecoxib obtained by quench-cooling of the melt is physically unstable and will easily recrystallize, below and above T_g. Grzybowska and coauthors[13] suggested that only the high fragility correlates with the large tendency of celecoxib to crystallize, and not the β_{KWW}, which corresponds to a relatively narrow distribution of relaxation times (and related to a small tendency to crystallization). A high value of fragility indicates that near T_g celecoxib exhibits a significant molecular mobility; the molecular motions associated to the structural α-relaxation and ultimately those related to the JG β-process (because it is the precursor of the α-relaxation) seem responsible for the low stability of amorphous celecoxib.[13]

In the present work, the relatively large degree of nonexponentiality and the high fragility index would both suggest that *S*-flurbiprofen has a great tendency to crystallize. Since *S*-flurbiprofen belongs to the same chemical family as ibuprofen, it is interesting to compare the dynamical behavior and physical stability of these two glass formers. The asymmetric α-relaxation spectra of ibuprofen are described by the same value of β_{KWW} (= 0.52), but the fragility index

estimated from the temperature evolution of the α-relaxation time is $m = 93 \pm 2$.[27] Thus, the higher fragility value here found for *S*-flurbiprofen ($m = 113 \pm 2$) could point toward a greater tendency to recrystallize than the less fragile ibuprofen. In fact, when flurbiprofen and ibuprofen are obtained in the amorphous form by cooling (at 10 K·min^{-1}) the liquid of their respective crystalline forms and submitting to the similar temperature variations like in a DSC experiment with cooling/heating cycles at 10 K·min^{-1}, cold-crystallization is observed starting at about 40 degrees above T_g upon heating *S*-flurbiprofen from the glassy state (recalling run 3 in Figure 4), while no crystallization is observed for ibuprofen.[27]

Before closing this subsection, it should be mentioned that the Vogel temperature, T_0, is far from being adequate to obtain information about the physical stability of an amorphous material. The present study clearly shows that the knowledge of T_0 alone cannot be used as a measure in predicting physical stability: for *S*-flurbiprofen it is found that $T_g - T_{0,1}$ is equal to 35 degrees suggesting that storage at temperatures 35 degrees below T_g would ensure stabilization of the amorphous solid (at those temperatures the VFTH model predicts the arrest of molecular motions associated to the α-relaxation). Nevertheless, the dielectric characterization of the glassy state here reported shows that localized motions with a relatively important intensity still persist in the glass (recognized as a JG β-process), being detectable at very low temperatures until at least 32 degrees below T_0, i.e., ∼70 degrees below T_g (recalling Figures 7 and 9). As already mentioned, studies of some glass formers including pharmaceuticals compounds[12,45] have shown that this kind of secondary relaxation is in the origin of nucleation/crystallization processes of the glassy state. Further studies are needed to check if the JG β-process, that is the precursor of the α-relaxation, also plays a role in the physical instability of amorphous *S*-flurbiprofen.

3.2.2.2. Analysis of dc Conductivity: Test of the Debye–Stokes–Einstein Relationship. At high temperatures, above 277 K, the dielectric loss curves ($\varepsilon''(f)$) are influenced by conductivity, which manifests in the low frequency side of the spectra (Figure 7c). It can be due to trace ionic impurities that migrate over extended trajectories between the electrodes[114] and/or intrinsic proton diffusion along hydrogen bonds.[23,31,32] The charge transport takes place due to hopping conduction accompanied by electrical relaxation whose contribution increases with decreasing frequency.[90] Information on this low frequency/high temperature effect can be obtained from the frequency dependence of the real part of conductivity, $\sigma'(f)$ (see Data Analysis section) shown in Figure 11 for amorphous *S*-flurbiprofen.

As it was found for a variety of quite different materials,[90,115−117] the $\sigma'(f)$ plot shows a transition from a plateau, due to pure dc conductivity at low frequencies (σ_{dc}), bending to a frequency-dependent conductivity (ac conductivity) at higher frequencies (which follows a power law $\sigma' \approx (2\pi f)^s$ with $s \leq 1$).[90,118] In *S*-flurbiprofen, the α-relaxation associated with the dynamic glass transition (285 K $\leq T \leq$ 303 K) also leads to a frequency-dependent regime of $\sigma'(f)$ but with a higher *s* exponent than for pure ac conductivity; this behavior is clearly shown in Figure 11 by comparison with the loss peak that emerges at the same frequency range, exemplified for data obtained at $T = 285$ K. It is important to note that the plateau region corresponds to a linear dependence of slope = −1 in the plots of $\log_{10}(\varepsilon''(f))$ versus $\log_{10}(f)$, which also allows obtaining the value of σ_{dc}; remember that in the fitting

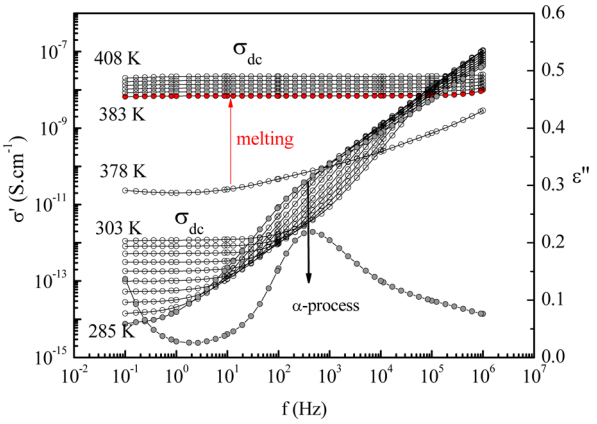

Figure 11. Left-hand axis: Frequency dependence of the real part of the conductivity, σ' (in log–log scale) obtained for amorphous *S*-flurbiprofen: between 285 and 303 K in steps of 2 degrees; from 383 to 408 K in steps of 5 degrees. Data obtained between 305 and 373 K is not shown since crystallization occurred; $\sigma'(f)$ obtained at 378 K is included allowing identification of melting. Right-hand axis: dielectric loss representation of the spectrum at 285 K evidencing the position of the α-process. Lines are guides to the eyes.

procedure of the dielectric spectra, a term $\sigma_{dc}/(\varepsilon_0\omega)$ was added to the imaginary part of the HN fitting function (eq 8) to take into account the dc conductivity contribution (global HN fittings curves shown in Figure 7c). For $T >$ 303 K cold-crystallization of the sample drastically changes the σ' spectra (not shown). After melting (curves above 378 K in Figure 11), $\sigma'(f)$ presents the behavior expected for a liquid.

The temperature dependence of dc conductivity values obtained from both $\sigma'(f)$ and $\varepsilon''(f)$ analysis is shown in Figure 12a (left-hand *yy*′-axis). As found for the α-relaxation time (right-hand *yy*′-axis), the temperature dependence of $\sigma_{dc}(T)$ is curved when plotted versus the temperature reciprocal: σ_{dc} slows down dramatically as the temperature decreases toward T_g, following a non-Arrhenian behavior. This kind of behavior of $\sigma_{dc}(T)$ has been found for a variety of glass formers.[31,70,71,115,117,119,120] It can be described by the empirical VFTH equation rewritten as

$$\sigma_{dc}(T) = \sigma_\infty \exp\left(-\frac{B_\sigma}{T - T_{0,\sigma}}\right) \quad (15)$$

where the pre-exponential term σ_∞ is the value at infinite temperature and B_σ and $T_{0,\sigma}$ are characteristics of the material. The fitting of this equation to the $\sigma_{dc}(T)$ data is shown in Figure 12a as solid black line, and the characteristic parameters are presented in Table 1.

A close inspection of Figure 12a reveals that at high temperatures (down to around 320 K) $\log_{10}\sigma_{dc}(T)$ versus $1/T$ runs nearly parallel to $-\log_{10}\tau_\alpha(T)$ vs $1/T$, but its curvature becomes different when the temperature decreases to T_g (note that the same axis scaling, i.e., decades per centimeter, is used for both data). This result points to a decoupling of ionic conductivity from structural relaxation approaching T_g.

According to the Debye–Stokes–Einstein equation (eq 6) that relates dc conductivity with the structural relaxation time, τ_α, a slope of −1 is predicted for the plot of $\log_{10}\sigma_{dc}$ versus $\log_{10}\tau_\alpha$, when the translational motions associated to conductivity and the orientational molecular motions controlling the structural relaxation are fully coupled; if breakdown of dynamics occurs, the FDSE relationship applies (eq 7) and the

dx.doi.org/10.1021/mp4002188 | *Mol. Pharmaceutics* 2014, 11, 112−130

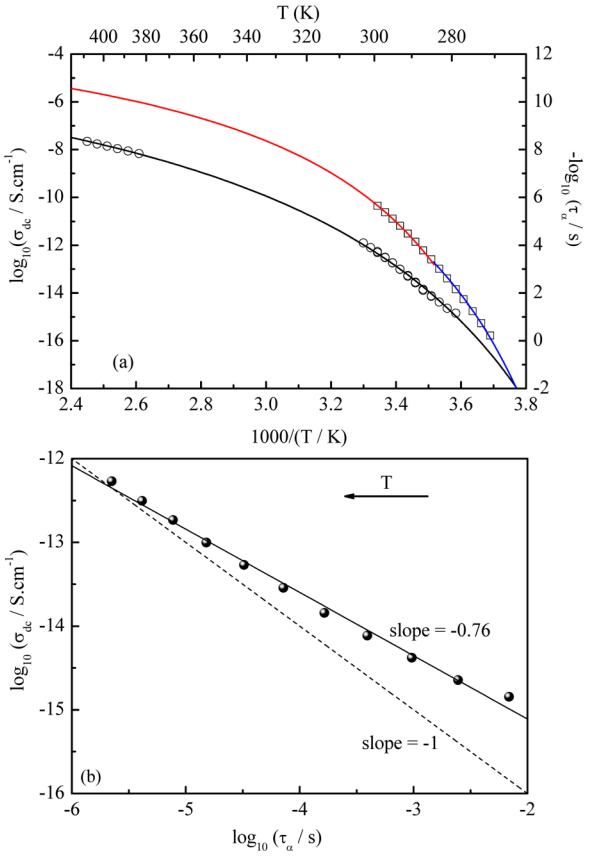

Figure 12. (a) Left-hand axis: temperature dependence of dc conductivity, σ_{dc}, of amorphous *S*-flurbiprofen (circles). Black line is the VFTH (eq 15) fit curve to $\sigma_{dc}(T)$. Right-hand axis: temperature dependence of the α-relaxation time (τ_α) including the two VFTH fitting curves, blue and red lines (see Figure 9). (b) Representation of log σ_{dc} versus log τ_α (filled circles) for temperatures close to T_g where both contributions are detected simultaneously (279 K $\leq T \leq$ 299 K). Dashed line (slope = −1) is the prevision from the DSE relationship (corresponding to x = 1, i.e., $\sigma_{dc}(T) \propto 1/\tau_\alpha(T)$ and taking into account that at high temperatures ($T = \infty$) $\tau_{\alpha,\infty} = 10^{-14}$ s and $\sigma_\infty = 1.0 \times 10^{-4}$ S·cm^{-1} (Table 1)). Black solid line is the linear fitting curve to $\log_{10} \sigma_{dc} = f(\log_{10} \tau_\alpha)$ data with slope = −0.76 = −x (x, the fractional exponent of the FDSE relationship $\sigma_{dc}(T) \propto 1/\tau_\alpha(T)^x$).

slope of $\log_{10} \sigma_{dc} = f(\log_{10} \tau_\alpha)$ is $-x$, with the fractional exponent $0 < x < 1$.

In order to test the validity of the Debye−Stokes−Einstein relationship, the plot of $\log_{10} \sigma_{dc}$ against $\log_{10} \tau_\alpha$ for *S*-flurbiprofen is shown in Figure 12b, at temperatures near T_g where both contributions are detected simultaneously (279 K $\leq T \leq$ 299 K); a straight line of slope −1 (= −x) is also drawn for comparison (dashed line): experimental data do not lie on this line, i.e., there is a breakdown of the DSE relationship for supercooled *S*-flurbiprofen at temperatures close to T_g. The linear fitting to the $\log_{10} \sigma_{dc} = f(\log_{10} \tau_\alpha)$ plot (solid line) allows estimating a fractional exponent of the FDSE relationship x = 0.76 ± 0.02. Commonly reported values for this fractional exponent are in the range from 0.75 to 0.91.[31,32,66,71] In conclusion, for *S*-flurbiprofen there is an enhancement of translational ionic motions in comparison with the orientational molecular motions as the glass transition temperature T_g is approached. A detailed discussion of this subject will be reported elsewhere.

4. CONCLUSIONS

Conventional DSC, TMDSC, and dielectric relaxation spectroscopy were used complementarily to show that crystallization of *S*-flurbiprofen can be circumvented on cooling from the molten state of its crystalline form exhibiting a glass transition $T_{g,onset\ (TMDSC,\ DRS)}$ = 265 K; it undergoes cold-crystallization on heating, melting at the same temperature as the as-received material ($T_{m,peak}$ = 384 K) leading to conclude that the same crystalline form is obtained upon recrystallization.

It was shown that the isochronal dielectric analysis (dielectric permittivity expressed as a function of temperature) in the temperature range between 183 and 408 K is suitable to characterize phase and thermal transitions associated with amorphous *S*-flurbiprofen allowing: (i) a direct visualization of the α-relaxation peak associated to the dynamic glass transition of the amorphous material, (ii) the precise determination of temperatures associated with crystallization and melting transitions, and (iii) the observation of secondary relaxation processes at temperatures below T_g, where localized motions persist that can have potential impact in the drug chemical and physical stability.

Moreover, it was shown that the analysis of the $\varepsilon'(T)$ data (not affected by conductivity) allows also obtaining some information about structure properties of the glass forming drug. All this information is obtained directly from the analysis of raw data not implying any data modeling. Therefore, it must be emphasized that dielectric measurements in isochronal mode can be used routinely for characterizing or quality control of pharmaceutical compounds.

Furthermore, it was shown that another advantage of the dielectric relaxation spectroscopy technique is the possibility of modeling data collected isothermally allowing a quantitative assessment of potentially practical parameters associated with the characteristics of relaxation processes in the glassy, supercooled, and molten states of *S*-flurbiprofen: dielectric strength, spectral shape, relaxation time, and conductivity. In particular, a relaxation map of amorphous *S*-flurbiprofen was drawn including the relaxations times for a secondary β-relaxation and the main α-process associated with the dynamic glass transition.

In the glassy state, the relaxation times of the β-relaxation present an Arrhenius temperature dependence that changes at T_g, leading to a higher apparent activation energy interpreted as a genuine Johari−Goldstein (JG) process of intermolecular origin, which is a fundamental characteristic of glass formation being regarded as a precursor of the α-process.

In the supercooled liquid state, the spectra are dominated by the α-relaxation characterized by a relatively large degree of nonexponentiality. The respective temperature dependence of relaxation times strongly departs from linearity, which is quantified by a high value of the fragility index m allowing to classify *S*-flurbiprofen as a fragile glass former.

The high fragility and/or the subglass mobility associated with the β-process may be in the origin of the high crystallization tendency of *S*-flurbiprofen. This is a subject that gained particular relevance within the pharmaceutical sciences regarding the drug physical stability and requires further investigation.

dx.doi.org/10.1021/mp4002188 | *Mol. Pharmaceutics* 2014, 11, 112−130

AUTHOR INFORMATION

Corresponding Author

*(N.T.C.) E-mail: nd.correia@fct.unl.pt or natalia.correia@univ-lille1.fr. Fax: (+33) 03 20 43 40 84. Phone: (+33) 03 20 33 59 02.

Notes

The authors declare no competing financial interest.

ACKNOWLEDGMENTS

N.T.C. thanks Dr. Dirk Wilmer from NOVOCONTROL Technologies GmbH und Co. KG, Germany, for the information about the Pt100 Ω sensor calibration. Financial support from Fundação para a Ciência e Tecnologia (FCT, Portugal) through the project PTDC/CTM/098979/2008 and the contract PEst-C/EQB/LA0006/2011 is acknowledged. M.T.V. acknowledges FCT for a postdoctoral grant SFRH/BPD/39691/2007. This work was also supported by the "INTERREG IVA 2mers seas zeeen cross border Cooperation Program 2007−2013".

REFERENCES

(1) Hancock, B. C.; Zografi, G. Characteristics and significance of the amorphous state in pharmaceutical systems. *J. Pharm. Sci.* **1997**, *86*, 1−12.

(2) Hancock, B. C.; Parks, M. What is the true solubility advantage for amorphous pharmaceuticals? *Pharm. Res.* **2000**, *17*, 397−404.

(3) Roberts, C. J.; DeBenedetti, P. G. Engineering pharmaceutical stability with amorphous solids. *AIChE J.* **2002**, *48*, 1140−1144.

(4) Zhou, D.; Zhang, G. G. Z.; Law, D.; Grant, D. J. W.; Schmitt, E. A. Physical stability of amorphous pharmaceuticals: Importance of configurational thermodynamic quantities and molecular mobility. *J. Pharm. Sci.* **2002**, *91*, 1863−1872.

(5) Craig, D. Q. M.; Royall, P. G.; Kett, V. L.; Hopton, M. L. The relevance of the amorphous state to pharmaceutical dosage forms: glassy drugs and freeze dried systems. *Int. J. Pharm.* **1999**, *179*, 179−207.

(6) Yu, L. Amorphous pharmaceutical solids: Preparation, characterization and stabilization. *Adv. Drug Delivery Rev.* **2001**, *48*, 27−42 and references therein.

(7) Andronis, V.; Zografi, G. The molecular mobility of supercooled amorphous indomethacin as a function of temperature and relative humidity. *Pharm. Res.* **1998**, *15*, 835−842.

(8) Shalaev, E.; Shalaeva, M.; Zografi, G. The effect of disorder on the chemical reactivity of an organic solid, tetraglycine methyl ester: change of the reaction mechanism. *J. Pharm. Sci.* **2002**, *91*, 584−594.

(9) Hancock, B. C.; Shamblin, S. L.; Zografi, G. Molecular mobility of amorphous pharmaceutical solids below their glass transition temperatures. *Pharm. Res.* **1995**, *12*, 799−806.

(10) Aso, Y.; Yoshioka, S.; Kojima, S. Relationship between the crystallization rates of amorphous nifedipine, phenobarbital, and flopropione, and their molecular mobility as measured by their enthalpy relaxation and ^{1}H NMR relaxation times. *J. Pharm. Sci.* **2000**, *89*, 408−416.

(11) Zhou, D.; Zhang, G. G. Z.; Law, D.; Grant, D. J. W.; Schmitt, E. A. Thermodynamics, molecular mobility and crystallization kinetics of amorphous griseofulvin. *Mol. Pharmaceutics* **2008**, *5*, 927−936.

(12) Bhattacharya, S.; Suryanarayanan, R. Local mobility in amorphous pharmaceuticals characterization and implications on stability. *J. Pharm. Sci.* **2009**, *98*, 2935−2953.

(13) Grzybowska, K.; Paluch, M.; Grzybowski, A.; Wojnarowska, Z.; Hawelek, L.; Kolodziejczyk, K.; Ngai, K. L. Molecular dynamics and physical stability of amorphous anti-inflammatory drug: celecoxib. *J. Phys. Chem. B* **2010**, *114*, 12792−12801.

(14) Shamblin, S. L.; Tang, X.; Chang, L.; Hancock, B. C.; Pikal, M. J. Characterization of the time scales of molecular motion in pharmaceutically important glasses. *J. Phys. Chem. B* **1999**, *103*, 4113−4121.

(15) Kremer, F.; Schönhals, A., Eds. *Broadband Dielectric Spectroscopy*; Springer Verlag: Berlin, Germany, 2003.

(16) Smith, G.; Duffy, A. P.; Shen, J.; Olliff, C. J. Dielectric relaxation spectroscopy and some applications in the pharmaceutical sciences. *J. Pharm. Sci.* **1995**, *84*, 1029−1044.

(17) Craig, D. Q. M. *Dielectric Analysis of Pharmaceutical Systems*; Taylor & Francis: London, U.K., 1995.

(18) He, R.; Craig, D. Q. M. An investigation into the thermal behaviour of an amorphous drug using low frequency dielectric spectroscopy and modulated temperature differential scanning calorimetry. *J. Pharm. Pharmacol.* **2001**, *53*, 41−48.

(19) Carpentier, L.; Decressain, R.; Desprez, S.; Descamps, M. Dynamics of the amorphous and crystalline α-,γ-phases of indomethacin. *J. Phys. Chem. B* **2006**, *110*, 457−464.

(20) Wojnarowska, Z.; Adrjanowicz, K.; Wlodarczyk, P.; Kaminska, E.; Kaminski, K.; Grzybowska, K.; Wrzalik, R.; Paluch, M.; Ngai, K. L. Broadband dielectric relaxation study at ambient and elevated pressure of molecular dynamics of pharmaceutical: indomethacin. *J. Phys. Chem. B* **2009**, *113*, 12536−12545.

(21) Johari, G. P.; Kim, S.; Shanker, R. M. Dielectric studies of molecular motions in amorphous solid and ultraviscous acetaminophen. *J. Pharm. Sci.* **2005**, *94*, 2207−2223.

(22) Nath, R.; El Goresy, T.; Geil, B.; Zimmermann, H.; Böhmer, R. Relaxation in the glass former acetylsalicylic acid studied by deuteron magnetic resonance and dielectric spectroscopy. *Phys. Rev. E.* **2006**, *74*, 021506.

(23) Johari, G. P.; Kim, S.; Shanker, R. M. Dielectric relaxation and crystallization of ultraviscous melt and glassy states of aspirin, ibuprofen, progesterone, and quinidine. *J. Pharm. Sci.* **2007**, *96*, 1159−1175.

(24) Carpentier, L.; Decressain, R.; De Gusseme, A.; Neves, C.; Descamps, M. Molecular mobility in glass forming fananserine: A dielectric, NMR, and TMDSC investigation. *Pharm. Res.* **2006**, *23*, 798−805.

(25) Kaminski, K.; Paluch, M.; Ziolo, J.; Ngai, K. L. Dielectric studies of molecular motions in glassy and liquid nicotine. *J. Phys.: Condens. Matter* **2006**, *18*, 5607−5615.

(26) Brás, A. R.; Dionísio, M.; Correia, N. T. Molecular motions in amorphous pharmaceuticals. *AIP Conf. Proc.* **2008**, *982*, 91−96.

(27) Brás, A. R.; Noronha, J. P.; Antunes, A. M. M.; Cardoso, M. M.; Schönhals, A.; Affouard, F.; Dionisio, M.; Correia, N. T. Molecular motions in amorphous ibuprofen as studied by broadband dielectric relaxation spectroscopy. *J. Phys. Chem. B* **2008**, *112*, 11087−11099.

(28) Adrjanowicz, K.; Kaminski, K.; Wojnarowska, Z.; Dulski, M.; Hawelek, L.; Pawlus, S.; Paluch, M.; Sawicki, W. Dielectric relaxation and crystallization kinetics of ibuprofen at ambient and elevated pressure. *J. Phys. Chem. B* **2010**, *114*, 6579−6593.

(29) Brás, A. R.; Merino, E. G.; Neves, P. D.; Fonseca, I. M.; Dionísio, M.; Schönhals, A.; Correia, N. T. Amorphous ibuprofen confined in nanostructured silica materials: a dynamical approach. *J. Phys. Chem. C* **2011**, *115*, 4616−4623.

(30) Dantuluri, A. K. R.; Amin, A.; Puri, V.; Bansal, A. K. Role of α-relaxation on crystallization of amorphous celecoxib above T_g probed by dielectric spectroscopy. *Mol. Pharmaceutics* **2011**, *8*, 814−822.

(31) Andersson, O.; Johari, G. P.; Shanker, R. M. Effect of pressure on molecular and ionic motions in ultraviscous acetaminophen-aspirin mixture. *J. Pharm. Sci.* **2006**, *95*, 2406−2418.

(32) Johari, G. P.; Andersson, O. On the nonlinear variation of dc conductivity with dielectric relaxation time. *J. Chem. Phys.* **2006**, *125* (124501), 1−7.

(33) El Goresy, T.; Bohmer, R. Dielectric study of the viscous and glassy states of a binary, nifedipine-based pharmaceutical alloy. *J. Non-Cryst. Solids* **2006**, *352*, 4459−4463.

(34) El Goresy, T.; Böhmer, R. Dielectric relaxation processes in solid and supercooled liquid solutions of acetaminophen and nifedipine. *J. Phys.: Condens. Matter* **2007**, *19*, 205134 (1−9).

(35) Johari, G. P.; Kim, S.; Shanker, R. M. Dielectric study of equimolar acetaminophen-aspirin, acetaminophen-quinidine, and benzoic acid-progesterone molecular alloys in the glass and ultraviscous states and their relevance to solubility and stability. *J. Pharm. Sci.* **2010**, *99*, 1358−1374.
(36) Alie, J.; Menegotto, J.; Cardon, P.; Duplaa, H.; Caron, A.; Lacabanne, C.; Bauer, M. Dielectric study of the molecular mobility and the isothermal crystallization kinetics of an amorphous pharmaceutical drug substance. *J. Pharm. Sci.* **2004**, *93*, 218−233.
(37) Koronen, O.; Bhugra, C.; Pikal, M. J. Correlation between molecular mobility and crystal growth of amorphous phenobarbital and phenobarbital with polyvinylpyrrolidone and L-proline. *J. Pharm. Sci.* **2008**, *97*, 3830−3841.
(38) Adrjanowicz, K.; Wojnarowska, Z.; Wlodarczyk, P.; Kaminski, K.; Paluch, M.; Mazgalski, J. Molecular mobility in liquid and glassy states of telmisartan (TEL) studied by broadband dielectric spectroscopy. *Eur. J. Pharm. Sci.* **2009**, *38*, 395−404.
(39) Adrjanowicz, K.; Zakowiecki, D.; Kaminski, K.; Hawelek, L.; Grzybowska, K.; Tarnacka, M.; Paluch, M.; Cal, K. Molecular dynamics in supercooled liquid and glassy states of antibiotics: azithromycin, clarithromycin and roxithromycin studied by dielectric spectroscopy. Advantages given by the amorphous state. *Mol. Pharmaceutics* **2012**, *9*, 1748−1763.
(40) Wojnarowska, Z.; Grzybowska, K.; Hawelek, L.; Swiety-Pospiech, A.; Masiewicz, E.; Paluch, M.; Sawicki, W.; Chmielewska, A.; Bujak, P.; Markowski, J. Molecular dynamics studies on the water mixtures of pharmaceutically important ionic liquid lidocaine HCl. *Mol. Pharmaceutics* **2012**, *9*, 1250−1261.
(41) Bhardwaj, S. P.; Arora, K. K.; Kwong, E.; Templeton, A.; Clas, S. D.; Suryanarayanan, R. Correlation between molecular mobility and physical stability of amorphous itraconazole. *Mol. Pharmaceutics* **2013**, *10*, 694−700.
(42) Debenedetti, P. G.; Stillinger, F. H. Supercooled liquids and the glass transition. *Nature* **2001**, *410*, 259−267.
(43) DeBenedetti, P. G. *Metastable Liquids: Concepts and Principles*; Princeton University Press: Princeton, NJ, 1997.
(44) Roland, C. M. Relaxation phenomena in vitrifying polymers and molecular liquids. *Macromolecules* **2010**, *43*, 7875−7890.
(45) Ngai, K. L. *Relaxation and Diffusion in Complex Systems*; Springer: New York, 2011.
(46) Vogel, H. The temperature dependence law of the viscosity of fluids. *Phys. Z.* **1921**, *22*, 645−646.
(47) Fulcher, G. S. Analysis of recent measurements of the viscosity of glasses. *J. Am. Ceram. Soc.* **1925**, *8*, 339−355.
(48) Tammann, G.; Hesse, W. The dependancy of viscosity on temperature in hypothermic liquids. *Z. Anorg. Allg. Chem.* **1926**, *156*, 245−257.
(49) Kauzmann, W. The nature of the glassy state and the behavior of liquids at low temperatures. *Chem. Rev.* **1948**, *43*, 219−256.
(50) Angell, C. A. In *Relaxations in Complex Systems*; Ngai, K. L., Wright, G. B., Eds.; National Technical Information Service, US Department of Commerce: Springfield, VA, 1985; p 1.
(51) Angell, C. A. Relaxation in liquids, polymers and plastic crystals: Strong/fragile patterns and problems. *J. Non-Cryst. Solids* **1991**, *131*−*133*, 13−31.
(52) Böhmer, R.; Ngai, K. L.; Angell, C. A.; Plazek, D. J. Nonexponential relaxations in strong and fragile glass formers. *J. Chem. Phys.* **1993**, *99*, 4201−4209.
(53) Ngai, K. L. Dynamic and thermodynamic properties of glass-forming substances. *J. Non-Cryst. Solids* **2000**, *275*, 7−51.
(54) Böhmer, R.; Angell, C. A. Correlations of the nonexponentiality and state dependence of mechanical relaxations with bond connectivity in Ge-As-Se supercooled liquids. *Phys. Rev. B* **1992**, *45*, 10091−10094.
(55) Hancock, B. C.; Shamblin, S. L. Molecular mobility of amorphous pharmaceuticals determined using differential scanning calorimetry. *Thermochim. Acta* **2001**, *380*, 95−107.
(56) Kohlrausch, R. Nachtrag uber die elastische Nachwirkung beim Cocon und Glasfaden, etc. *Pogg. Ann. Phys (III)* **1847**, *12*, 393−399. Kohlrausch, R. Theorie des electrischen Ruckstandes in der Leidener Flasche. *Pogg. Ann. Phys (IV)* **1854**, *1*, 79−86.
(57) Williams, G.; Watts, D. C. Non-symmetrical dielectric relaxation behaviour arising from a simple empirical decay function. *Trans. Faraday Soc.* **1970**, *66*, 80−85.
(58) Shamblin, S. L.; Hancock, B. C.; Dupuis, Y.; Pikal, M. J. Interpretation of relaxation time constants for amorphous pharmaceutical systems. *J. Pharm. Sci.* **2000**, *89*, 417−427.
(59) Ngai, K. L. Relation between some secondary relaxations and the α relaxations in glass-forming materials according to the coupling model. *J. Chem. Phys.* **1998**, *109*, 6982−6994.
(60) Johari, G. P.; Goldstein, M. Viscous liquids and the glass transition. II. Secondary relaxations in glasses of rigid molecules. *J. Chem. Phys.* **1970**, *53*, 2372−2388; Viscous Liquids and the Glass Transition. III. Secondary relaxations in aliphatic alcohols and other nonrigid Molecules. *J. Chem. Phys.* **1971**, *55*, 4245−4252.
(61) Ngai, K. L. An extended coupling model description of the evolution of dynamics with time in supercooled liquids and ionic conductors. *J. Phys.: Condens. Matter* **2003**, *15*, S1107−S1125.
(62) Ngai, K. L.; Kamińska, E.; Sekuła, M.; Paluch, M. Primary and secondary relaxations in bis-5-hydroxypentylphthalate revisited. *J. Chem. Phys.* **2005**, *123*, 204507.
(63) Ngai, K. L.; Paluch, M. Classification of secondary relaxation in glass-formers based on dynamic properties. *J. Chem. Phys.* **2004**, *120*, 857−873.
(64) Angell, C. A.; Ngai, K. L.; McKenna, G. B.; McMillan, P. F.; Martin, S. W. Relaxation in glass-forming liquids and amorphous solids. *J. Appl. Phys.* **2000**, *88*, 3113−3157.
(65) Ngai, K. L.; Magill, J. H.; Plazek, D. J. Flow, diffusion and crystallization of supercooled liquids: Revisited. *J. Chem. Phys.* **2000**, *112*, 1887−1892.
(66) Roland, C. M.; Bielowka, S. H.; Paluch, M.; Casalini, R. Supercooled dynamics of glass-forming liquids and polymers under hydrostatic pressure. *Rep. Prog. Phys.* **2005**, *68*, 1405−1478.
(67) Ediger, M. D.; Harrowell, P. Perspective: Supercooled liquids and glasses. *J. Chem. Phys.* **2012**, *137*, 080901.
(68) Ediger, M. D.; Harrowell, P.; Yu, L. Crystal growth kinetics exhibit a fragility-dependent decoupling from viscosity. *J. Chem. Phys.* **2008**, *128*, 034709.
(69) Ngai, K. L. The vestige of many-body dynamics in relaxation of glass-forming substances and other interacting systems. *Philos. Mag.* **2007**, *87*, 357−370.
(70) Stickel, F.; Fischer, E. W.; Richert, R. Dynamics of glass-forming liquids. II. Detailed comparison of dielectric relaxation, dc conductivity, and viscosity data. *J. Chem. Phys.* **1996**, *104*, 2043−2055.
(71) Corezzi, S.; Campani, E.; Rolla, P. A.; Fioretto, D. Changes in the dynamics of supercooled systems revealed by dielectric spectroscopy. *J. Chem. Phys.* **1999**, *111*, 9343−9351.
(72) Hensel-Bielowka, S.; Psurek, T.; Ziolo, J.; Paluch, M. Test of the fractional Debye−Stokes−Einstein equation in low-molecular-weight glass-forming liquids under condition of high compression. *Phys. Rev. E* **2001**, *63*, 062301.
(73) Pawlus, S.; Paluch, M.; Sekula, M.; Ngai, K. L.; Rzoska, S. J.; Ziolo, J. Changes in dynamic crossover with temperature and pressure in glass-forming diethyl phthalate. *Phys. Rev. E* **2003**, *68*, 021503.
(74) Agapov, A. L.; Sokolov, A. P. Decoupling ionic conductivity from structural relaxation: a way to solid polymer electrolytes? *Macromolecules* **2011**, *44*, 4410−4414.
(75) Ngai, K. L. On enhanced translational diffusion or the fractional Stokes−Einstein relation observed in a supercooled ionic liquid. *J. Phys. Chem. B* **2006**, *110*, 26211−26214.
(76) Power, G.; Vij, J. K.; Johari, G. P. Structure-sependent DC conductivity and relaxation time in the Debye−Stokes−Einstein equation. *J. Phys. Chem. B* **2007**, *111*, 11201−11208.
(77) Bhugra, C.; Pikal, M. J. Role of thermodynamic, molecular, and kinetic factors in crystallization from the amorphous state. *J. Pharm. Sci.* **2008**, *97*, 1329−1349.

(78) Laitinen, R.; Löbmann, K.; Strachan, C. J.; Grohganz, H.; Rades, T. Emerging trends in the stabilization of amorphous drugs. *Int. J. Pharm.* **2012**, *453*, 65−79.
(79) Andronis, V.; Zografi, G. Crystal nucleation and growth of indomethacin polymorphs from the amorphous state. *J. Non-Cryst. Sol.* **2000**, *271*, 236−248.
(80) Rao, C. N. R.; Rao, K. J. *Phase Transitions in Solids*; McGraw-Hill: New York, 1978.
(81) Owen, A. E. *Amorphous Solids and the Liquid State*; Plenum: New York, 1985.
(82) Fokin, V. M.; Schmelzer, J. W. P.; Nascimento, M. L. F.; Zanotto, E. D. Diffusion coefficients for crystal nucleation and growth in deeply undercooled glass-forming liquids. *J. Chem. Phys.* **2007**, *126*, 234507 (1−6).
(83) Kelton, K. F. Crystal nucleation in liquids and glasses. *Solid State Phys.* **1991**, *45*, 75−177.
(84) Brittain, H. G., Ed. *Profiles of Drug Substances, Excipients and Related Methodology*, 1st ed.; Academic Press Elsevier Inc: Amsterdam, The Netherlands, 2012; Vol. *37*.
(85) Hensel, A.; Dobbertin, J.; Schawe, J. E. K.; Boller, A.; Schick, C. Temperature modulated calorimetry and dielectric spectroscopy in the glass transition region of polymers. *J. Therm. Anal.* **1996**, *46*, 935−954.
(86) Mano, J. F.; Lanceros-Méndez, S.; Nunes, A. M.; Dionísio, M. Temperature calibration in dielectric measurements. *J. Therm. Anal. Calorim.* **2001**, *65*, 37−49.
(87) Dionísio, M.; Mano, J. F. Dielectric Techniques. In *Handbook of Thermal Analysis and Calorimetry. Vol 5: Recent Advances, Techniques an Applications*; Brown, M. E.; Gallagher, P. K., Eds.; Elsevier: Amsterdam, The Netherlands, 2008; Chapter 7.
(88) Havriliak, S.; Negami, S. A complex plane representation of dielectric and mechanical relaxation processes in some polymers. *Polymer* **1967**, *8*, 161−210; A complex plane analysis of alpha-dispersions in some polymer systems. *J. Polym. Sci. C* **1966**, *14*, 99−117. recently revised in Havriliak, S. Jr.; Havriliak, S. *Dielectric and Mechanical Relaxation in Material*; Hanser: Munich, Germany, 1997.
(89) Schönhals, A.; Kremer, F. Analysis of Dielectric Spectra. In *Broadband Dielectric Spectroscopy*; Kremer, F., Schönhals, A., Eds.; Springer Verlag: Berlin, Germany, 2003; Chapter 3.
(90) Kremer, F.; Rozanski, S. A.The Dielectric Properties of Semiconducting Disordered Materials. In *Broadband Dielectric Spectroscopy*; Kremer, F., Schönhals, A., Eds.; Springer Verlag: Berlin, Germany, 2003; Chapter 12.
(91) Paradkar, A.; Maheshwari, M.; Tyagi, A. K.; Chauhan, B.; Kadam, S. S. Preparation and characterization of flurbiprofen beads by melt solidification technique. *AAPS PharmSciTech* **2003**, *4* (4), 65.
(92) Lefort, R.; De Gusseme, A.; Willart, J.-F.; Danède, F.; Descamps, M. Solid state NMR and DSC methods for quantifying the amorphous content in solid dosage forms: an application to ball-milling of trehalose. *Int. J. Pharm.* **2004**, *280*, 209−219.
(93) Viciosa, M. T.; Correia, N. T.; Salmerón Sanchez, M.; Carvalho, A. L.; Romão, M. J.; Gómez Ribelles, J. L.; Dionísio, M. Real-time monitoring of molecular dynamics of ethylene glycol dimethacrylate glass former. *J. Phys. Chem. B* **2009**, *113*, 14209−14217.
(94) Bustin, O.; Descamps, M. Slow structural relaxations of glass-forming maltitol by modulated DSC calorimetry. *J. Chem. Phys.* **1999**, *110*, 10982−10992.
(95) Viciosa, M. T.; Correia, N. T.; Salmerón Sanchez, M.; Gómez Ribelles, J. L.; Dionísio, M. Molecular dynamics of ethylene glycol dimethacrylate glass former: Influence of different crystallization pathways. *J. Phys. Chem. B* **2009**, *113*, 14196−14208.
(96) Merino, E. G.; Rodrigues, C.; Viciosa, M. T.; Melo, C.; Sotomayor, J.; Dionísio, M.; Correia, N. T. Phase transformations undergone by triton X-100 probed by differential scanning calorimetry and dielectric relaxation spectroscopy. *J. Phys. Chem. B* **2011**, *115*, 12336−12347.
(97) Massalska-Arodz, M.; Williams, G.; Smith, I. K.; Conolly, C.; Aldridge, G. A.; Dabrowski, R. Molecular dynamics and crystallization behaviour of isopentyl cyanobiphenyl as studied by dielectric relaxation spectroscopy. *J. Chem. Soc., Faraday Trans.* **1998**, *94*, 387−394.
(98) Böttcher, C. J. F. *Theory of Dielectric Polarization*; Elsevier: Amsterdam, The Netherlands, 1973; Vol. *1*. Böttcher, C. J. F.; Bordewijk, P. *Theory of Dielectric Polarization*; Elsevier: Amsterdam, The Netherlands, 1978; Vol. *2*; and references therein.
(99) Kudlik, A.; Tschirwitz, C.; Blochowicz, T.; Benkhof, S.; Rössler, E. Slow secondary relaxation in simple glass formers. *J. Non-Cryst. Solids* **1998**, *235−237*, 406−411.
(100) Ngai, K. L.; Capaccioli, S. Relation between the activation energy of the Johari−Goldstein β relaxation and T_g of Glass Formers. *Phys. Rev. E* **2004**, *69*, 031051 (1−5).
(101) Schönhals, A. Dielectric Properties of Amorphous Polymers. In *Dielectric Spectroscopy of Polymeric Materials*; Runt, J., Fitzgerald, J., Eds; ACS Books: Washington, DC, 1997.
(102) Schönhals, A. Molecular Dynamics in Polymer Model Systems. In *Broadband Dielectric Spectroscopy*; Kremer, F., Schönhals, A., Eds.; Springer Verlag: Berlin, Germany, 2003; Chapter 7.
(103) Kremer, F.; Schönhals, A. The Scaling of the Dynamics of Glasses and Superccoled Liquids. In *Broadband Dielectric Spectroscopy*; Kremer, F., Schönhals, A., Eds.; Springer Verlag: Berlin, Germany, 2003; Chapter 4; and references therein.
(104) Schönhals, A.; Kremer, F. Theory of Dielectric Relaxation. In *Broadband Dielectric Spectroscopy*; Kremer, F., Schönhals, A., Eds.; Springer Verlag: Berlin, Germany, 2002; Chapter 1.
(105) Rengarajan, G. T.; Beiner, M. Relaxation behavior and crystallization kinetics of amorphous acetaminophen. *Lett. Drug Des. Discovery* **2006**, *3*, 723−730.
(106) Massalska-Arodz, M.; Williams, G.; Thomas, D. K.; Jones, W. J.; Dabrowski, R. Molecular dynamics and crystallization behavior of chiral isooctyloxycyanobiphenyl as studied by dielectric relaxation spectroscopy. *J. Phys. Chem. B* **1999**, *103*, 4197−4205.
(107) León, C.; Ngai, K. L. Rapidity of the change of the kohlrausch exponent of the α-relaxation of glass-forming liquids at T_B or T_β and consequences. *J. Phys. Chem. B* **1999**, *103*, 4045−4051.
(108) Casalini, R.; Ngai, K. L.; Roland, C. M. Connection between the high-frequency crossover of the temperature dependence of the relaxation time and the change of intermolecular coupling in glass-forming liquids. *Phys. Rev. B* **2003**, 014201.
(109) Stickel, F.; Fischer, E. W.; Richert, R. Dynamics of glass-forming liquids. I. Temperature-derivative analysis of dielectric relaxation data. *J. Chem. Phys.* **1995**, *102*, 6251−6257.
(110) Corezzi, S.; Beiner, M.; Huth, H.; Schröter, K.; Fioretto, D.; Donth, E. Two crossover regions in the dynamics of glass forming epoxy resins. *J. Chem. Phys.* **2002**, *117*, 2435−2448.
(111) Schönhals, A.; Schick, C.; Huth, H.; Frick, B.; Mayorova, M.; Zorn, R. Molecular dynamics in glass-forming poly(phenyl methyl siloxane) as investigated by broadband thermal, dielectric and neutron spectroscopy. *J. Non-Cryst. Solids* **2007**, *353*, 3853−3861.
(112) Ngai, K. L.; Lunkenheimer, P.; León, C.; Schneider, U.; Brand, R.; Loidl, A. Nature and properties of the Johari−Goldstein β-relaxation in the equilibrium liquid state of a class of glass-formers. *J. Chem. Phys.* **2001**, *115*, 1405−1413.
(113) Beiner, M. Relaxation in poly(alkyl methacrylate)s: Crossover region and nanophase separation. *Macromol. Rapid Commun.* **2001**, *22*, 869−895.
(114) Jonscher, A. K. Dielectric relaxation in solids. *J. Phys. D: Appl. Phys.* **1999**, *32*, R57−R70.
(115) Sun, M.; Pejanović, S.; Mijović., J. Dynamics of deoxyribonucleic acid solutions as studied by dielectric relaxation spectroscopy and dynamic mechanical spectroscopy. *Macromolecules* **2005**, *38*, 9854−9864.
(116) Neagu, E.; Pissis, P.; Apekis, L.; Gómez Ribelles, J. L. Dielectric relaxation spectroscopy of polyethylene terephthalate (PET) films. *J. Phys. D: Appl. Phys.* **1997**, *30*, 1551−1560.
(117) Lu, H.; Zhang, X.; Zhang, H. Influence of the relaxation of Maxwell−Wagner−Sillars polarization and dc conductivity on the dielectric behaviors of nylon 1010. *J. Appl. Phys.* **2006**, *100*, 054104.

(118) Jonscher, A. K. The 'universal' dielectric response. *Nature* **1977**, *267*, 673−679.
(119) Bauer, T.; Köhler, M.; Lunkenheimer, P.; Loidl, A.; Angell, C. A. Relaxation dynamics and ionic conductivity in a fragile plastic crystal. *J. Chem. Phys.* **2010**, *133*, 144509.
(120) Leys, J.; Wübbenhorst, M.; Menon, C. P.; Rajesh, R.; Thoen, J.; Glorieux, C.; Nockemann, P.; Thijs, B.; Binnemans, K.; Longuemart, S. Temperature dependence of the electrical conductivity of imidazolium ionic liquids. *J. Chem. Phys.* **2008**, *128*, 064509.